Biochemistry -- Faculty Publications

Biochemistry, Department of

2003

THE MANY FACES OF VITAMIN B12: CATALYSIS BY COBALAMIN-DEPENDENT ENZYMES

Ruma Banerjee

Stephen W. Ragsdale

THE MANY FACES OF VITAMIN B_{12}: CATALYSIS BY COBALAMIN-DEPENDENT ENZYMES[1]

Ruma Banerjee and Stephen W. Ragsdale

*Department of Biochemistry, University of Nebraska, Lincoln, Nebraska 68588-0664;
email:rbanerjee1@unl.edu; sragsdale1@unl.edu*

Key Words   cobalamin, methyltransferase, dehalogenase, isomerase, adenosylcobalamin, methylcobalamin, methanogenesis, acetogenesis, homocysteine, methionine, adenosylmethionine

■ **Abstract**   Vitamin B_{12} is a complex organometallic cofactor associated with three subfamilies of enzymes: the adenosylcobalamin-dependent isomerases, the methylcobalamin-dependent methyltransferases, and the dehalogenases. Different chemical aspects of the cofactor are exploited during catalysis by the isomerases and the methyltransferases. Thus, the cobalt-carbon bond ruptures homolytically in the isomerases, whereas it is cleaved heterolytically in the methyltransferases. The reaction mechanism of the dehalogenases, the most recently discovered class of B_{12} enzymes, is poorly understood. Over the past decade our understanding of the reaction mechanisms of B_{12} enzymes has been greatly enhanced by the availability of large amounts of enzyme that have afforded detailed structure-function studies, and these recent advances are the subject of this review.

CONTENTS

---

[1]Abbreviations used: MeCbl, methylcobalamin; AdoCbl, 5′ deoxyadenosyl cobalamin; CH_3-H_4folate, methyltetrahydrofolate; CH_3-H_4MPT: methyltetrahydromethanopterin; CoM, Coenzyme M or mercaptoethanesulfonate; CODH, carbon monoxide dehydrogenase; ACS, acetyl-CoA synthase; AdoMet, S-adenosylmethionine; CFeSP, corrinoid iron-sulfur protein; PCB, polychlorinated biphenyl.

INTRODUCTION

The history of vitamin B_{12}, originating in 1925 with the descriptions by Whipple and Minot & Murphy of the antipernicious anemia factor, is rich and replete with scientific milestones (1, 2). A hunt spanning two decades led independently to the isolation of the cofactor by Smith & Folkers in 1948 and dramatically changed the therapeutic solution for pernicious anemia from several grams of uncooked liver to a few micrograms of a red crystalline compound (3, 4)! Solution of the crystal structure of vitamin B_{12} by Hodgkin in 1956 (5) and an intense transatlantic collaboration culminating in the total synthesis of the cofactor involving the Woodward and Eschenmoser laboratories were some of the other highlights of the ensuing decades (5a).

Vitamin B_{12} is a tetrapyrrolic cofactor in which the central cobalt atom is coordinated by four equatorial nitrogen ligands donated by pyrroles A-D of the corrin ring. B_{12} is portly and, unlike other tetrapyrroles, has a built-in axial ligand appended from the periphery of ring D of the corrin macrocycle (Figure 1). The identity of the base at the terminus of the propanolamine tether varies in different organisms and is the unusual ribonucleoside, dimethylbenzimidazole, found in cobalamins. Diversity is also present at the upper axial ligand where cyano-, methyl-, and deoxyadenosyl-groups are seen in vitamin B_{12}, methylcobalamin (MeCbl[1]), and AdoCbl or coenzyme B_{12} respectively.

As major strides were being made on elucidating the identity and structure of the antipernicious anemia factor, a biological role for B_{12} was unraveled in Barker's laboratory where an AdoCbl derivative was found to be the cofactor for glutamate mutase (6). This was followed by the discovery several years later of the other biologically active alkylcobalamin, MeCbl (7). Presently, three classes of B_{12} enzymes are recognized, the isomerases, the methyltransferases, and the reductive dehalogenases. Recent advances in our understanding of their reaction mechanisms are the subject of this review.
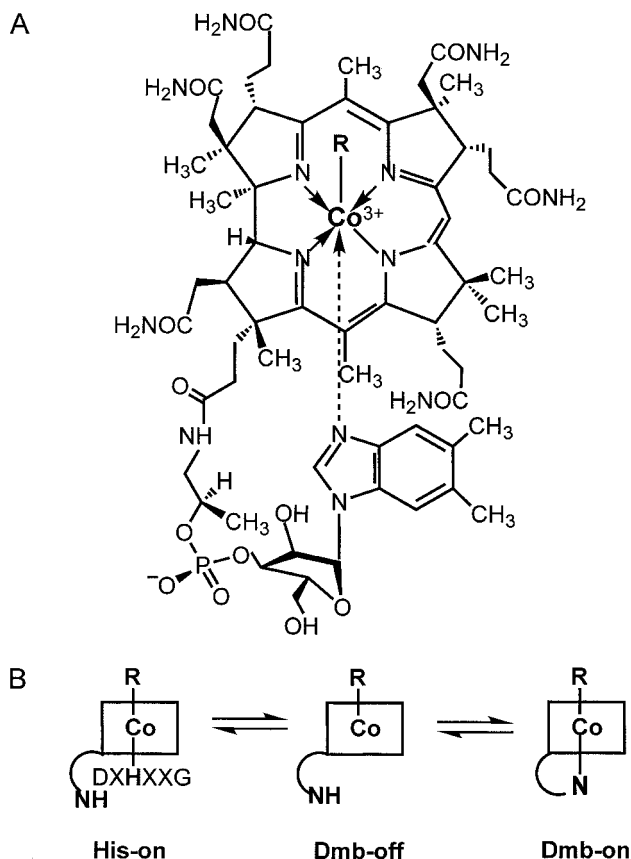
A

B

His-on   Dmb-off   Dmb-on

Figure 1   Structure and alternative conformations of cobalamin found in B$_{12}$-dependent enzymes. (*A*) Structure of cobalamin, where R is deoxyadenosine in AdoCbl, methyl in MeCbl, -OH in hydroxocobalamin, and -CN in vitamin B$_{12}$. (*B*) The free cofactor can exist in the base-on (or Dmb-on) or base-off (or Dmb-off) conformations, with the former predominating at physiological pH. The His-on conformation in which the endogenous ligand, dimethylbenzimidazole, is replaced by an active site histidine is seen is some B$_{12}$-dependent enzymes. In the corrinoid iron-sulfur (CFeSP) protein, the cofactor is in the base-off conformation, and a protein ligand does not appear to occupy the lower axial position.

B$_{12}$-DEPENDENT ISOMERASES

The isomerases are the largest subfamily of B$_{12}$-dependent enzymes found in bacteria, where they play important roles in fermentation pathways (8–10). The only exception is methylmalonyl-CoA mutase, which is found in both bacteria and in man. In some organisms, a B$_{12}$-dependent ribonucleotide reductase
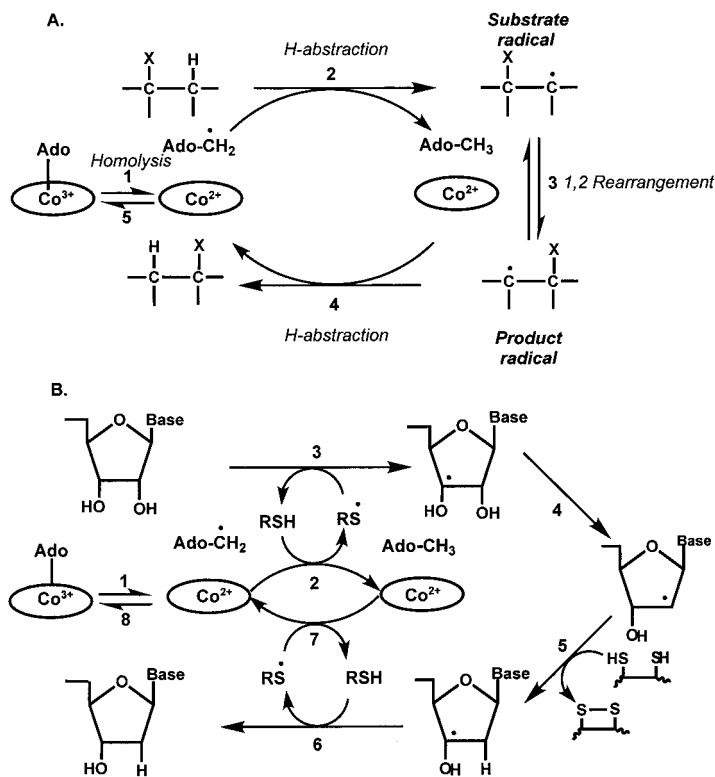
Figure 2 (*A*) General reaction mechanism for AdoCbl-dependent isomerases. (*B*) In class II ribonucleotide reductases, a thiyl radical rather than the initially formed 5′-deoxyadenosyl radical abstracts a hydrogen atom from the substrate and reduction occurs at C2′ of the substrate.

catalyzes the conversion of ribonucleotides to deoxyribonucleotides, which is fundamentally important for DNA replication and repair. B_{12}-dependent isomerases catalyze the 1,2 interchange between a variable substituent and a hydrogen atom on vicinal carbons (Figure 2). Considerable diversity exists in the nature of the migrating group ranging from carbon (in methylmalonyl-CoA mutase, isobutyryl-CoA mutase, glutamate mutase, and methyleneglutarate mutase) to nitrogen (in ethanolamine ammonia lyase, D-ornithine aminomutase, and β-lysine mutase) and oxygen (in diol dehydrase).

Subclasses of Isomerases

Recent crystal structures and spectroscopic studies have led to the recognition of two subclasses of B_{12}-dependent enzymes that differ with respect to their mode

of cofactor binding (Figure 1). In solution and at physiological pH, the lower ligand position is occupied by the endogenous base, dimethylbenzimidazole, in a conformation that has been referred to in the literature as base-on. Protonation of the lower base, which has a pKa of 3.7 in AdoCbl (11), leads to the base-off conformer. Crystal structures of the Class I or His-on family of B$_{12}$-dependent isomerases have revealed the presence of yet another cofactor conformation in which the lower axial ligand, dimethylbenzimidazole, is replaced by a histidine residue donated by the protein (12, 13). The histidine is embedded in a D**XH**XX**G** sequence, which is the only primary sequence motif that appears to be conserved in both the B$_{12}$-dependent isomerase and methyltransferase family members that use the same cofactor-binding mode (14). In this mode, the nucleotide tail is bound in an extended conformation that results in dimethyl-benzimidazole being >10Å removed from the cobalt to which it is coordinated in solution. The isomerases in this subfamily include methylmalonyl-CoA mutase, glutamate mutase, methyleneglutarate mutase, isobutyryl-CoA mutase, and lysine 5,6 aminomutase.

In the Class II or Dmb-on family of B$_{12}$-dependent isomerases, the solution conformation of the cofactor is retained upon binding to the active site. Thus, dimethylbenzimidazole is coordinated to the cobalt in the lower axial position. This mode of B$_{12}$ binding has been seen in the crystal structures of diol dehydratase (15) and ribonucleotide reductase (16) and is expected for ethanolamine ammonia lyase based on the electron paramagnetic resonance (EPR) spectra (17, 18).

Despite the differences in the conformations of the bound cofactor, the B$_{12}$-dependent isomerases, with the exception of ribonucleotide reductase, exhibit similarities in the structural motifs they employ (Figure 3). A TIM barrel is juxtaposed on the upper face of cobalamin and encases the active site where the substrate binds. Numerous hydrogen bonds extend between the peripheral side chains on the corrin ring and the protein and likely contribute to the tight binding of the cofactor. In methylmalonyl-CoA mutase (12) and in glutamate mutase (13), the lower face of cobalamin is perched on the carboxy-terminal end of a Rossman (α/β)-fold, and a histidine residue extends from a loop to coordinate to the cobalt. In diol dehydratase, a Rossman-fold like structure exists in the central part of the β-subunit, which cups the lower face of the cofactor and may be important in making contact with the nucleotide (15). In contrast, ribonucleotide reductase exhibits a novel fold for binding B$_{12}$, which is more similar to the related structural elements used in the diiron-tyrosyl radical-dependent ribonucleotide reductases than it is to other B$_{12}$ enzymes (16).

Cofactor Is a Latent Radical Reservoir

The organometallic bond in AdoCbl is water stable but is relatively weak with a bond dissociation energy estimated to be 31.5 kcal mol^{-1} for the base-on conformer and 34.5 kcal mol^{-1} for the base-off conformer (19–21). The inherent lability of the Co-carbon bond is exploited by AdoCbl-dependent isomerases to
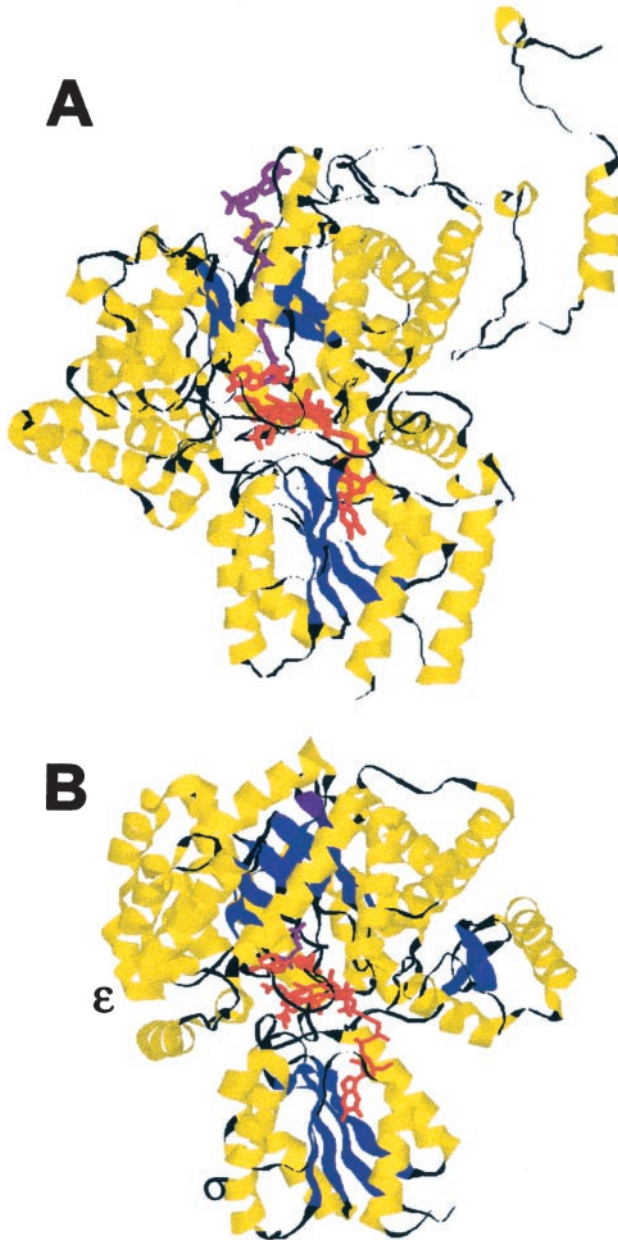
Figure 3 Comparison of the B$_{12}$-binding domains of AdoCbl-dependent isomerases: *A*, methylmalonyl-CoA mutase; *B*, glutamate mutase; *C*, dioldehydratase; and *D*, ribonucle-otide reductase.
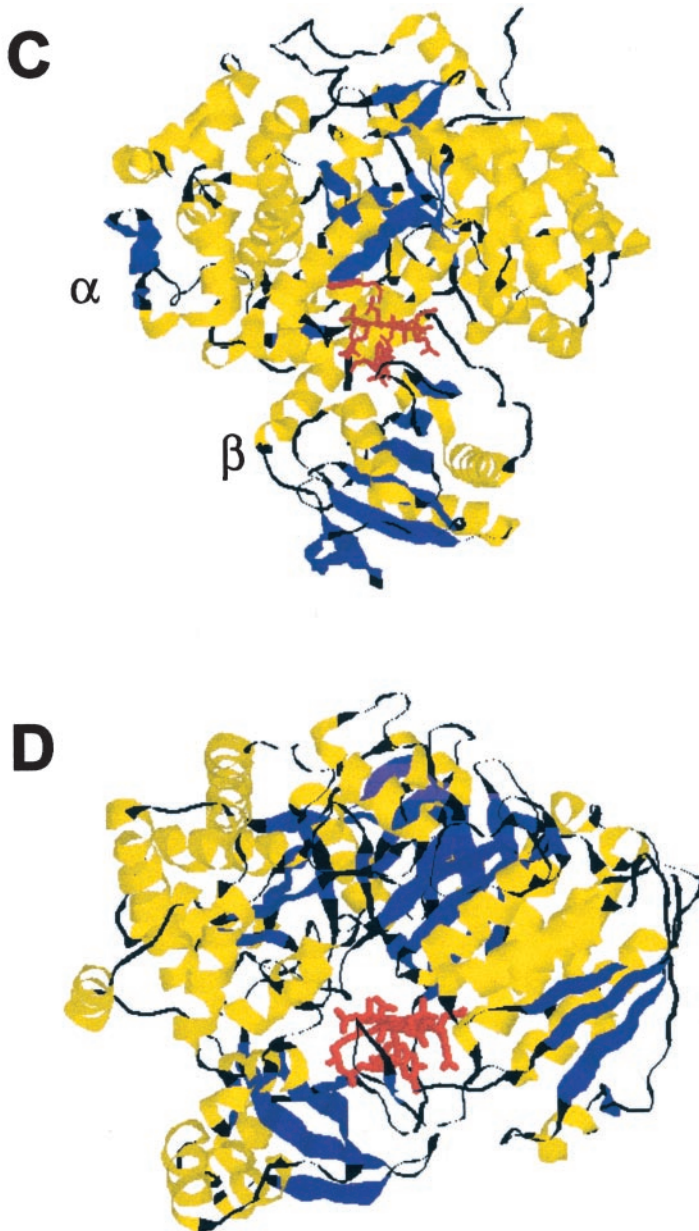
C

α

β

D

Figure 3   *Continued.*

effect radical based rearrangements that are initiated by homolysis of the Co-carbon bond (22). In the absence of substrate, the homolysis products, cob(II)alamin and the deoxyadenosyl radical, are not observed, indicating that the equilibrium for the homolysis reaction greatly favors geminate recombination. However, in the presence of substrate, the radical reservoir is mobilized into action as evidenced by an approximately trillionfold acceleration of the homolytic cleavage rate compared to the uncatalyzed rate in solution (20). Thus, utilization of substrate binding energy is key to controlling the homolysis equilibrium and protecting the latent radical pool from dissipation in side reactions.

Although ground state destabilization of the Co-carbon bond had been considered as a strategy for achieving the trillionfold homolysis rate enhancement (23–26), it is mechanistically unappealing. Stabilization of the deoxyadenosyl radical in the absence of substrate would lead to its rapid extinction and accumulation of inactive enzymes in the aerobic milieu where most of these enzymes operate. The extent of ground state stabilization has been experimentally evaluated by resonance Raman studies on methylmalonyl-CoA mutase in which isotope editing was employed to identify the Co-carbon stretching frequency for the free and enzyme-bound cofactor (27). The difference in their positions (6 cm^{-1}) was estimated to correspond to ~0.5 kcal mol^{-1} weakening of the Co-carbon bond, which is miniscule compared to the ~17 kcal mol^{-1} that occurs during the catalytic cycle (27). Resonance Raman spectra of glutamate mutase have also been reported (28); however, in the absence of isotope editing, conclusions regarding the identity and location of the Co-carbon stretching frequency can not be made.

Homolysis Timing Control

A key control issue for AdoCbl-dependent radical enzymes is containing the reactivity of the radical reservoir to minimize inactivating side reactions of the homolysis products. Insights into how this control is achieved have emerged from kinetic and mutagenesis studies on these enzymes. Propagation of the organic radical from deoxyadenosine to substrate is believed to occur directly in these enzymes with the exception of ribonucleotide reductase where an intermediate protein based cysteinyl radical is generated and operates as the working radical (Figure 2). The homolysis rate has been estimated in several of these enzymes by stopped-flow kinetic measurements and in each case found to be rapid and not rate limiting for catalytic turnover. A curious observation, first made with methylmalonyl-CoA mutase and later with other enzymes, was that the rate of cofactor homolysis is sensitive to isotopic substitution in the substrate (29). Thus, substitution of protiated methylmalonyl-CoA with [CD$_3$]-methylmalonyl-CoA decelerated homolysis ~20-fold at 25°C (29, 30). Similarly, use of the corresponding deuterated substrates led to substantial slowing of the homolysis rates in glutatmate mutase (31) and in ethanolamine ammonia lyase (32). These observations were curious not only because of the sensitivity of bond cleavage in
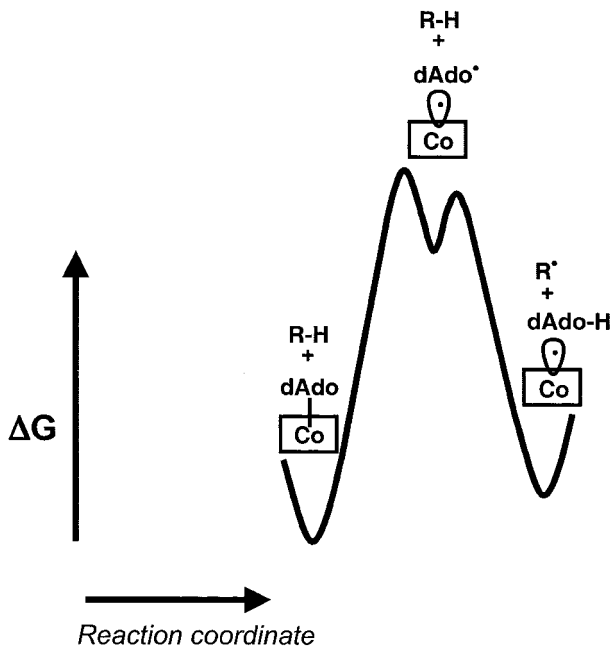
Figure 4   Qualitative free energy profile demonstrating kinetic coupling as a strategy for controlling the timing of the homolysis reaction.

the cofactor to isotopic substitution in the substrate, but also because the magnitude of the isotopic discrimination was anomalous and outside the range predicted for semiclassical behavior.

These results were interpreted as evidence for kinetic coupling between the homolytic cleavage and substrate radical generation steps as shown in Figure 4. According to this model, the homolysis equilibrium is unfavorable and lies in the direction of geminate recombination. However, in the presence of substrate, the high-energy dAdo•intermediate abstracts a hydrogen atom from the substrate to generate a more stable substrate-centered radical. The net effect of this coupled reaction is a shift in the overall homolysis equilibrium from recombination to radical propagation. This model provides an explanation for the sensitivity of the homolysis step to isotopic substitution in the substrate. Because detectable accumulation of the homolysis product, cob(II)alamin, is dependent on the generation of the substrate radical, its rate of formation is sensitive to whether a hydrogen or deuterium atom is being abstracted.

In ribonucleotide reductase, kinetic coupling involves generation of a thiyl radical rather than a substrate radical by the deoxyadenosyl radical (33). A working thiyl radical is common to both the diiron-tryosyl radical-dependent and B$_{12}$-dependent ribonucleotide reductases, and it is responsible in turn for generating the substrate radical. Mutation of C408, the site of the thiyl radical in the

Lactobacillus leichmannii B_{12}-dependent ribonucleotide reductase, leads to failure of the mutant enzyme to catalyze Co-carbon bond homolysis (33).

The basis of the anomalously large isotope effects has been characterized by examining the temperature dependence of the isotope effect in methylmalonyl-CoA mutase (30). The deuterium isotope effect increases from 35.6 to 49.9 as the temperature decreases from 20°C to 5°C. The magnitude of the isotope effect on the Arrhenius preexponentials (0.078) and the difference in the activation energies (Ea_D-Ea_H = 3.41 kcal mol^{-1}) deviate significantly from the values predicted for semiclassical behavior and provide strong evidence for quantum mechanical tunneling. Exalted tritium isotope effects of the order of 80–110 have been reported for diol dehydratase (34) and ethanolamine ammonia lyase (35, 36), and it is likely that nonclassical transfer pathways are involved in hydrogen atom abstraction by these enzymes as well.

Control of Radical Trajectories

One of the challenges for enzymes that deploy radical chemistry is the danger of extinction of reactive intermediates lurking in active sites lined with potential hydrogen atom donors. This problem is magnified in B_{12}-dependent isomerases where significant distances are bridged as the organic radical propagates intermolecularly between deoxyadenosine and substrate. EPR spectroscopy reveals the presence of biradical intermediates, which are either strongly or weakly coupled depending on whether the interradical distance is moderate (5–7Å) or large (10–11Å) (37). In most cases, the organic radical has been assigned as being either substrate- or product-derived, based on isotopic perturbation of the EPR spectra. The deoxyadenosyl radical has eluded detection in AdoCbl-dependent enzymes consistent with the kinetic coupling model in which it is not predicted to accumulate.

Depending on the interradical distance, the interaction between cob(II)alamin and the organic radical is either strong or weak as evidenced by the very different EPR spectral morphologies seen in B_{12}-dependent isomerases. In diol dehydratase and in ethanolamine ammonia lyase, a doublet signal is seen in spectra that consist of a broad resonance near $g = 2.3$ [due to cob(II)alamin] and a doublet of lines split by 70–140 Gauss near $g = 2.0$. The doublet signal arises from the organic radical split by weak isotropic exchange and dipolar coupling interactions with cob(II)alamin (38, 39). Simulations yield an electron-electron distance of ~10Å, which is consistent with the crystal structure of diol dehydratase (15).

In contrast, ribonucleotide reductase (40), glutamate mutase (41), methylene-glutarate mutase (42, 43), and methylmalonyl-CoA mutase (44, 45) exhibit EPR spectra with very different characteristics and have an effective g value of ~2.1 and resolved cobalt hyperfine splittings with ~55 G spacing. This class of EPR spectra arise from strong interactions between cob(II)alamin and the radical species via exchange and dipolar interactions (37). Simulations yield an electron-electron distance of 5–7Å for the spectra associated with ribonucleotide
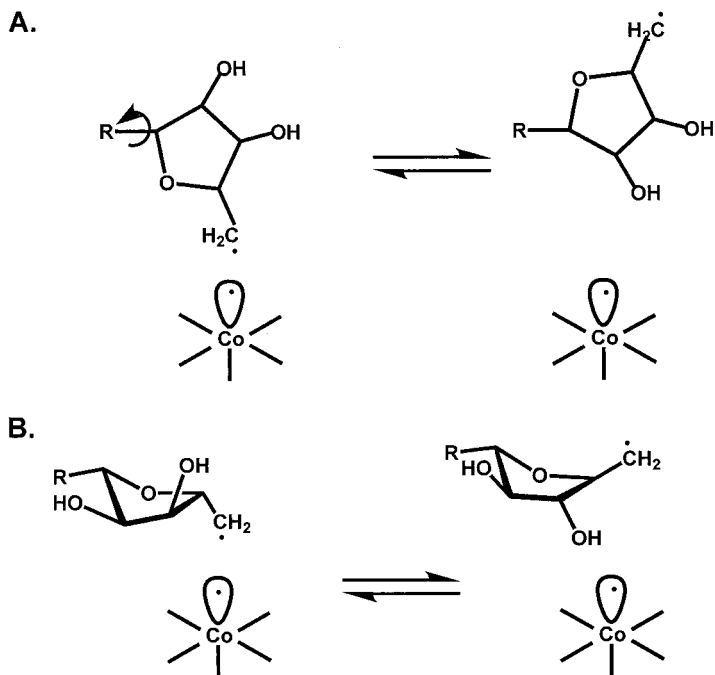
Figure 5   Ribose conformations control radical trajectories during propagation steps in diol dehydratase (*A*) and in glutamate mutase (*B*).

reductase (46) and glutamate mutase (41), which is consistent with the crystal structures of these enzymes (13, 16). In ribonucleotide reductase, a thiyl radical coupled to cob(II)alamin has been observed and was identified by substitution of the protons on the β-carbon of cysteine, which resulted in spectral narrowing (40).

The EPR spectra reveal that significant distances are traversed as the organic radical propagates between deoxyadenosine and substrate/product during each catalytic cycle, and this raises the issue of how side reactions are suppressed. Insights into how these enzymes control radical trajectories have emerged from structures of diol dehydratase (47) and glutamate mutase (48). In both cases, conformational toggling of the deoxyadenosine radical results in its reorientation from one favoring recombination to one abutting the substrate hydrogen atom destined for abstraction. In glutamate mutase, the interradical distance between the substrate and cob(II)alamin is estimated to be $\sim$6.6Å by simulations of the EPR spectra (41). This distance is bridged by a pseudorotation of the ribose ring that moves the C5′ carbon (where the radical is localized) from an axial to an equatorial location and thereby guides the radical away from geminate recombination and toward substrate radical generation (Figure 5). The crystal structure of glutamate mutase shows a mixed population of conformers, C2′-*endo* (C5′ is

positioned above the cobalt) and C3′-*endo* (C5′ is directed toward the substrate) (48).

A different movement, i.e., rotation around the N-glycosidic bond, swings the C5′ radical in diol dehydratase away from cob(II)alamin and toward the substrate (Figure 5) (47). This rather large movement accomplishes the transfer of the organic radical over an ~7Å distance from its original position in the spin-correlated radical pair to within van der Waal's contact distance of the substrate hydrogen atom destined for abstraction has been monitored in ethanolamine ammonia lyase by electron nuclear double resonance (49) and electron spin echo envelope modulation spectroscopy (50). Together, these studies provide fascinating glimpses into strategies adopted by B_{12}-dependent enzymes for controlling radical trajectories and stereospecificity of hydrogen atom abstraction.

Rearrangement Mechanisms

The differences in the chemical reactivities of the groups that are rearranged by B_{12}-dependent isomerases have necessitated the reliance on different strategies for achieving their rearrangements (Figure 6). Crystal structure determinations combined with computational studies have played a synergistic role in guiding mutational and kinetic studies aimed at understanding the mechanisms of rearrangement. In this section, isomerizations catalyzed by diol dehydratase, methylmalonyl-CoA mutase, and glutamate mutase are discussed in detail as prototypes for rearrangement mechanisms for B_{12}-dependent isomerases.

In diol dehydratase, an active site potassium coordinates to the two hydroxyl groups of the substrate that replace two water molecules in the resting enzyme (Figure 6). It is seven-coordinate with the remaining ligands being supplied by the protein (15). Experiments with ^{18}O-labeled propane 1,2 diols have demonstrated that the oxygen atom that is eliminated is derived from the O1 or O2 hydroxyl depending on the chirality at C2 of the substrate (51). These results necessitate the formation of a 1,1 gem-diol as an obligatory intermediate in the dehydration of propanediol and, in analogy, of ethanediol catalyzed by diol dehydratase.

Computational studies have been conducted to examine the energetics for alternative pathways for rearrangement (52–54). A transition state for migration was found only for the concerted mechanism but not for the stepwise pathway in which the hydroxyl group dissociates from C2 before adding to C1 (52). Ab initio studies have led to the proposal of a retro-push-pull mechanism in which the migration barrier is reduced by a combination of partial protonation and deprotonation of the migrating and spectator hydroxyl groups respectively (53). Candidate active site residues that could participate in such a mechanism are E170, positioned for pull catalysis with respect to the spectator hydroxyl, and H143, poised for retro-push catalysis via hydrogen bonding to the migrating hydroxyl (Figure 6). Potassium, whose Lewis acidity is expected to be diminished by the seven oxygen atoms surrounding it in the active site, appears to be

chiefly important in binding and orienting the substrate rather than in lowering the migration barrier (53, 54).

Polar radical pathways are also predicted for the carbon skeleton rearrangements catalyzed by methylmalonyl-CoA mutase and glutamate mutase. However, a key difference between the two reactions is the migration of an sp^2-hybridized carbon in methylmalonyl-CoA mutase and an sp^3 center in glutamate mutase. For the methylmalonyl-CoA mutase-catalyzed reaction, both fragmentation/recombination and intramolecular addition/elimination pathways can be entertained. However, computational studies indicate that the energetic barrier for the intramolecular pathway is lower than for the dissociative pathway and reveal that partial proton transfer to the migrating group would facilitate rearrangement (55, 56). H244 is positioned in the active site of methylmalonyl-CoA mutase to serve as a general acid and engage in a hydrogen bonding interaction with the substrate carbonyl group (Figure 6). Mutation of H244 (to glycine, alanine, or glutamine) results in a 10^2-10^3-fold decrease in kcat and loss of one of the two kinetic pKa's seen in the wild-type enzyme (57, 58). The overall integrity of the mutant enzyme is confirmed in the crystal structure of the H244A mutant, which is superimposable on that of the wild-type enzyme (58). The impact of the H244 mutation on rearrangement was evaluated by monitoring the ratio of tritium partitioned from the 5′ position of AdoCbl to substrate and product as a function of which was used to initiate this reversible isomerization reaction (58). The partition ratio was altered with respect to wild-type enzyme and was sensitive to the direction of the reaction in contrast to the reaction catalyzed by the wild-type enzyme. These results indicate that a catalytic penalty incurred by mutation of H244 is an increase in the rearrangement barrier. Interestingly mutation of this residue greatly enhances the oxidative sensitivity and leads to frequent interception of cob(II)alamin during the reaction indicating that H244 plays a key role in protecting radical intermediates (57, 58).

Glutamate mutase is the only known carbon skeleton isomerase in which a saturated carbon moiety undergoes migration. A cyclic intramolecular pathway is chemically implausible for this reaction, while a fragmentation/recombination route is feasible. Rapid quench flow studies have provided evidence for the formation of a glycyl radical and acrylate at kinetically competent rates, although the amount of these species detected was very low (59). Ab initio molecular orbital calculations predict that the fragmentation barrier for a neutral substrate is significantly lower than for one in which the glutamyl radical is either deprotonated or protonated (60). Three arginine residues interact with the two carboxylate groups while E171 is within hydrogen bonding distance to the α-amino group of the substrate in the active site of glutamate mutase (Figure 6). Mutation of E171 to glutamine decreases kcat 50-fold and alters the pH profile for Vmax (61). In addition, the overall deuterium isotope effect decreases from $^DV = 4.6$ in wild type to 2.1 in the mutant, which indicates that some other step contributes more significantly to limiting the reaction rate in the mutant. Together, these data are consistent with a role for the glutamate residue as a
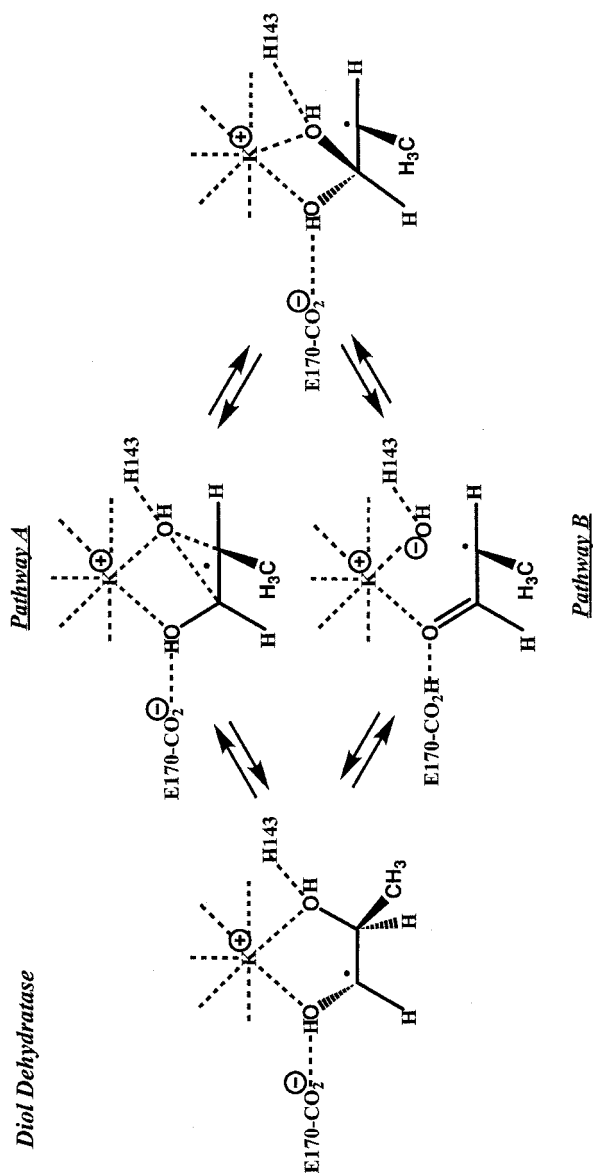
Figure 6 Alternative pathways for the rearrangement reactions in representative members of AdoCbl-dependent isomerases.
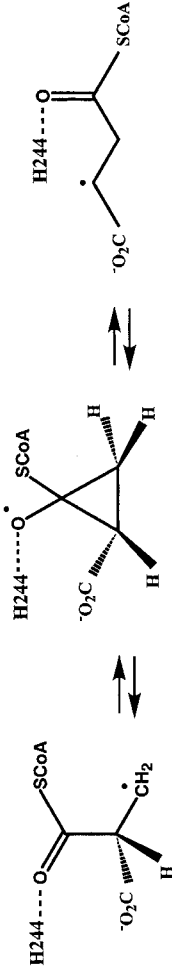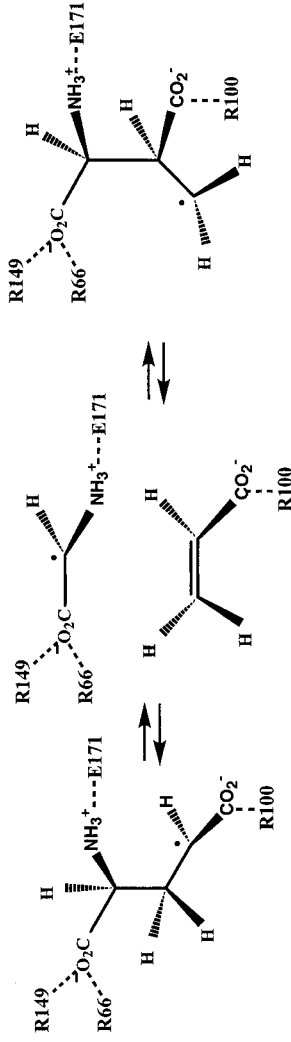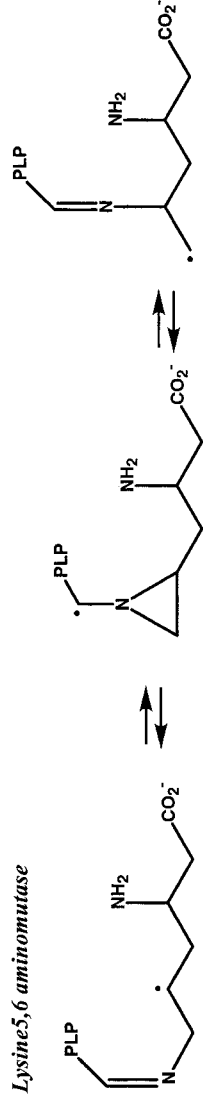
Methylmalonyl-CoA mutase

Glutamate mutase

Lysine5,6 aminomutase

Figure 6 *Continued.*

general base that deprotonates the α-amino group and facilitates the rearrangement reaction.

In the subclass of aminomutases encompassing D-lysine 5,6 aminomutase (62) and D-ornithine aminomutase (63), an entirely different strategy is employed for stabilization of the migrating group. These enzymes are dependent on pyridoxal phosphate, and the amino group of the substrate forms a Schiff base with this cofactor. The resulting sp^2 hybridized amino group can then undergo rearrangement via an intramolecular addition/elimination pathway (64). Computational studies predict that protonation of the pyridoxal phosphate ring would enhance the reaction via captodative stabilization of the cyclic intermediate (65).

Although the strategies deployed by B_{12}-dependent enzymes to orchestrate the approximately trillion fold rate acceleration in cleavage of the Co-carbon bond has been the focus of much attention, an equally amazing facet of these reactions is the magnitude of stabilization afforded for reactive carbon radical intermediates. Mutagenesis studies guided by crystal structures, in concert with computational studies, are beginning to illuminate this issue and reveal the roles of active site residues in stabilizing intermediates and facilitating the rearrangement reaction.

Mechanism-Based Inactivation and Reactivation of Isomerases

B_{12}-dependent isomerases exhibit both substrate-induced and oxygen-dependent lability, which leads to the gradual accumulation of inactive enzyme during turnover. The relative susceptibilities of these enzymes to inactivation vary over at least 8 orders of magnitude, from 0.7 min^{-1} in lysine 5,6 aminomutase (66) to $\sim 4 \times 10^{-8}$ min^{-1} in methylmalonyl-CoA mutase [estimated from data in (58)]. In the latter enzyme, inactivation is dependent on the presence of oxygen and, although the mechanism has not been investigated, presumably results from interception of cob(II)alamin and/or the organic radical by oxygen during catalytic turnover.

Substrate-dependent inactivation of lysine 5,6 aminomutase does not require the presence of oxygen. Interestingly in this enzyme, radical extinction occurs by intermolecular electron transfer from cob(II)alamin to either the substrate or product radical. This leads to the formation of oxidized, cob(III)alamin and a carbanion that is rapidly quenched by protonation. Similar mechanism-based inactivation has been observed with substrate and cofactor analogs in other systems (67, 68). Substrate-dependent inactivation has also been observed in diol dehydratase and glycerol dehydratase, but the mechanism has not been elucidated (69–71).

Because glycerol dehydratase and its isofunctional enzyme, diol dehydrate, play an essential role in glycerol fermentation in some bacteria, their propensity to undergo substrate-induced inactivation poses a conundrum. A clue to the existence of a repair system came from the demonstration that glycerol-inactivated enzymes in permeabilized bacterial cells are rapidly reactivated by the
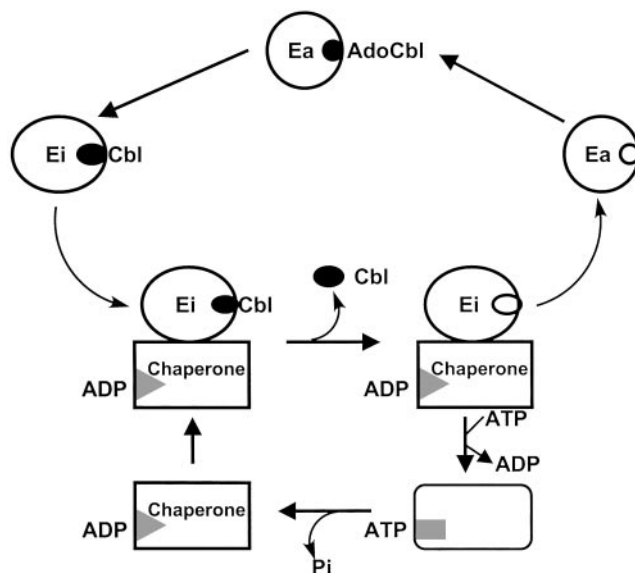
Figure 7 Postulated mechanism of reactivation of diol dehydratase by an ATP-dependent chaperone.

exchange of modified cofactor for intact AdoCbl in the presence of ATP and Mg^{2+} (72, 73). This in turn led to the discovery of a class of B$_{12}$ chaperones that function to release inactive cofactor from their target isomerases and regenerate apoenzyme that can be reloaded with AdoCbl (Figure 7) (74, 75).

The chaperone for diol dehydratase has been best characterized and exists as an $\alpha_2\beta_2$ complex (76). It exhibits low intrinsic ATPase activity and forms a tight complex with diol dehydratase and ADP. It is in this complex that inactive cofactor is eliminated from the isomerase and binding of ATP results in dissociation of the chaperone-target enzyme pair. The resulting apoenzyme can bind AdoCbl to form active holoenzyme.

B$_{12}$-DEPENDENT METHYLTRANSFERASES

The B$_{12}$-dependent methyltransferases play an important role in amino acid metabolism in many organisms (including humans) as well as in one-carbon metabolism and CO$_2$ fixation in anaerobic microbes. In this section, we describe the general characteristics of methyltransferase reactions, then discuss specific methyltransferases and their metabolic roles, and conclude with a discussion of their reaction mechanism.

Figure 8 Methyl donors and acceptors used by the B_{12}-dependent methyltransferases. B_{12}-dependent methyltransferases catalyze the 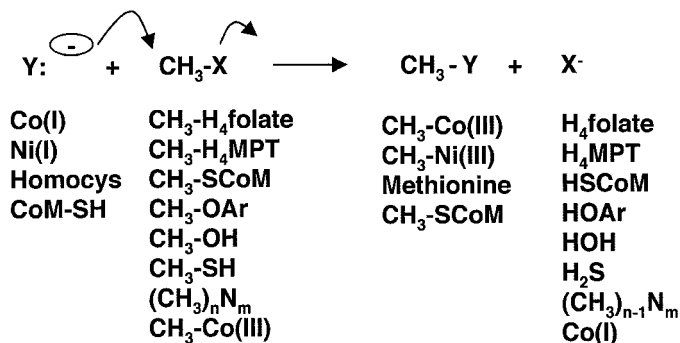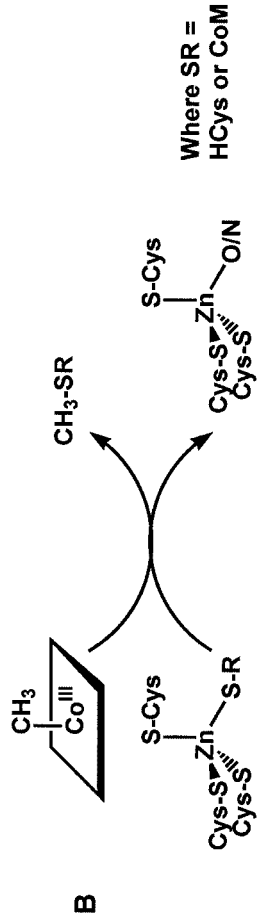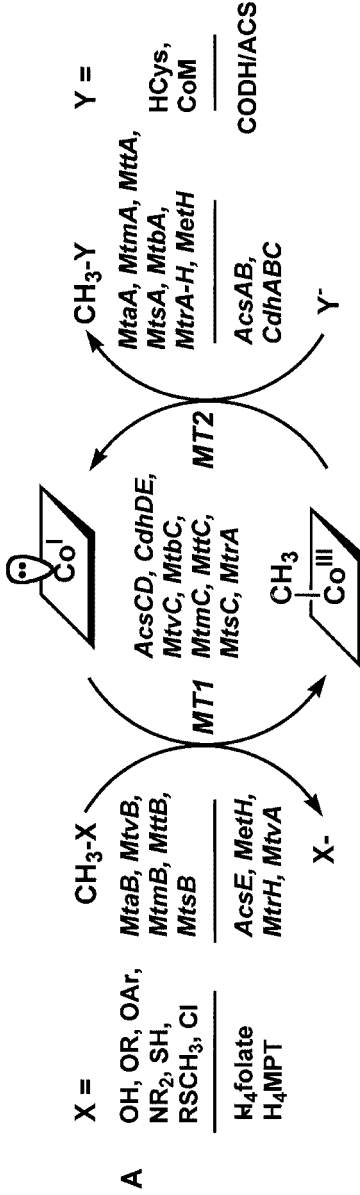movement of a methyl group from a methyl donor (X-CH$_3$) to a methyl group acceptor (Nuc), where X and Nuc are the leaving group and the nucleophile, respectively.

Classes of B_{12}-Dependent Methyltransferases

As a subclass of the group transfer enzymes, B_{12}-dependent methyltransferases catalyze the movement of a methyl group from a methyl donor to a methyl group acceptor (Figure 8), where X and Nuc are the leaving group and the nucleophile, respectively. Three components are required for the methyl transfer reaction, and each component is found on a different polypeptide or domain (Figure 9). A specific three-component system is utilized for each methyl donor. A B_{12}-containing protein alternatively undergoes methylation by an MT1-component, which binds the methyl donor (CH$_3$-X), and demethylation by an MT2 component, which binds the final methyl group acceptor (Y).

There are two MT1 classes: one subclass binds simple substrates like methanol (MtaB), methylated amines (MttB, MtbB, MtmB), methylated thiols (MtsB), methoxylated aromatics (MtvB), and methylated heavy metals, while the

→

Figure 9 Three components of the B_{12}-dependent methyltransferases. Three components are required for the methyl transfer reaction; each component is found on a different polypeptide or domain. Mt designates methyltransferase, while the third letter denotes the methyl donor (a, methanol; v, vanillate; m, methylamine; t, trimethylamine; and s, dimethylsulfide). Acs designates that the protein is a component of the acetyl-CoA synthase (ACS) operon, with AB denoting the CODH/ACS, CD the two subunits of the CFeSP, and E the methyltetrahydrofolate:CFeSP MeTr. The last letter designates the specific component: *B* methylates the corrinoid protein, *C* is the corrinoid protein, and *A* methylates CoM. Thus, B_{12}-containing protein (*Mt_C*) alternatively undergoes methylation by a *MT1*- or *Mt_B*- component, which binds and activates the methyl donor, and demethylation by a *MT2* or *Mt_A* homolog that binds the final methyl group acceptor.

A

X =

OH, OR, OAr,
NR$_2$, SH,
RSCH$_3$, Cl

H$_4$folate
H$_4$MPT

CH$_3$-X

MtaB, MtvB,
MtmB, MttB,
MtsB

AcsE, MetH,
MrtH, MtvA

MT1

AcsCD, CdhDE,
MtvC, MtbC,
MtmC, MttC,
MtsC, MtrA

Co^I Co^{III}—CH$_3$

X-

CH$_3$-Y

MtaA, MtmA, MttA,
MtsA, MtbA,
MtrA-H, MetH

AcsAB,
CdhABC

MT2

Y-

Y =

HCys,
CoM

CODH/ACS

B

CH$_3$—Co^{III}

Cys-S
Cys-S—Zn—S-R
       S-Cys

CH$_3$-SR

Cys-S
Cys-S—Zn—O/N
       S-Cys

Where SR =
HCys or CoM

other catalyzes methyl transfer from CH_3-H_4folate (AcsE-MeTr) and the methanogenic analog, methyltetrahydromethanopterin (CH_3-H_4MPT). Transfer of a methyl group from MT1 to the second B_{12}-containing component leads to formation of an organometallic methylcobalt intermediate. The third component (MT2) catalyzes transfer of the Co-bound methyl group to an acceptor (e.g., CoM, acetyl-CoA synthase, and H_4MPT). All the MT2-type enzymes isolated so far contain Zn, which coordinates to and thereby activates the thiolate methyl acceptor (Figure 9B). The methyl transfer to CODH/ACS involves a different type of reaction in which the methyl group appears to be transferred from cobalt to nickel.

Methionine Synthase

Methionine synthase from *Escherichia coli* (MetH) is the most extensively studied B_{12}-dependent methyltransferase. It catalyzes transfer of the methyl group from CH_3-H_4folate to homocysteine to form methionine and H_4folate (Figure 10) (77–78a). Compared to model reactions, methyl transfer from enzyme-bound CH_3-H_4folate to Co(I) is accelerated 35-million-fold and, from CH_3-Co(III) to bound homocysteine, 6-million-fold (77). Methionine synthase is a modular enzyme containing separate binding domains for homocysteine, CH_3-H_4folate, B_{12}, and AdoMet (79) (Figure 11). The B_{12} domain in its different oxidation states must interact punctually and specifically with each of the other three domains: The Co(I) form with the CH_3-H_4folate binding domain, the Co(II) form with the AdoMet binding domain, and the CH_3-Co(III) form with the homocysteine binding domain. The various conformational changes required to accomplish this molecular juggling act apparently are rate limiting during steady-state turnover (77).

The independently expressed modules of methionine synthase retain most of the functional properties of the native protein (79). A serendipitous proteolytic cleavage of methionine synthase in the crystallization process excised the B_{12} binding domain, which led to the first crystal structure of a protein-bound B_{12} (80). Surprisingly, cobalamin binding is accompanied by replacement of the lower axial benzimidazole ligand by a histidine residue to generate the His-on conformation (Figure 1B). The histidine residue is part of a catalytic triad consisting of H759, D757, and S810 that controls the coordination state of cobalt, i.e., His-on or His-off, by modulating the protonation state of the histidine.

Methyltransferases Involved in Anaerobic CO_2 Fixation and Energy Metabolism

Derivatives of B_{12} play key roles in energy metabolism and in cell carbon synthesis in anaerobic microbes such as methanogenic archaea (81) and acetogenic bacteria (82).

ACETOGENESIS AND B_{12} Acetogenic bacteria are important in the carbon cycle for degrading a wide variety of compounds derived from lignin and complex
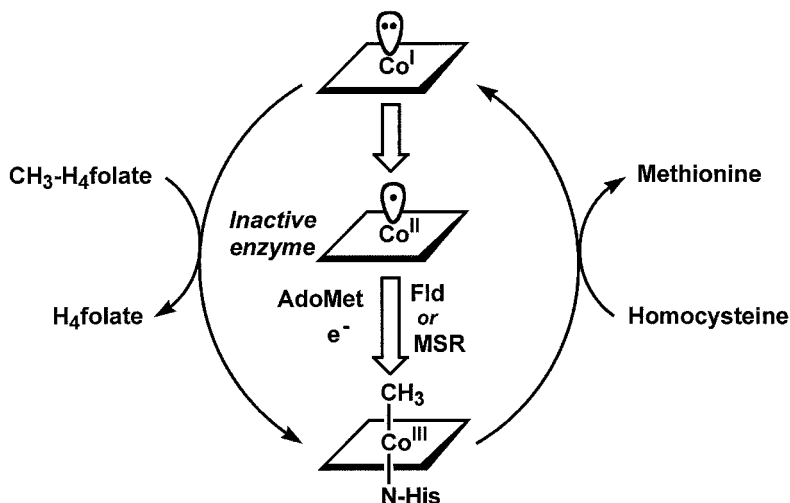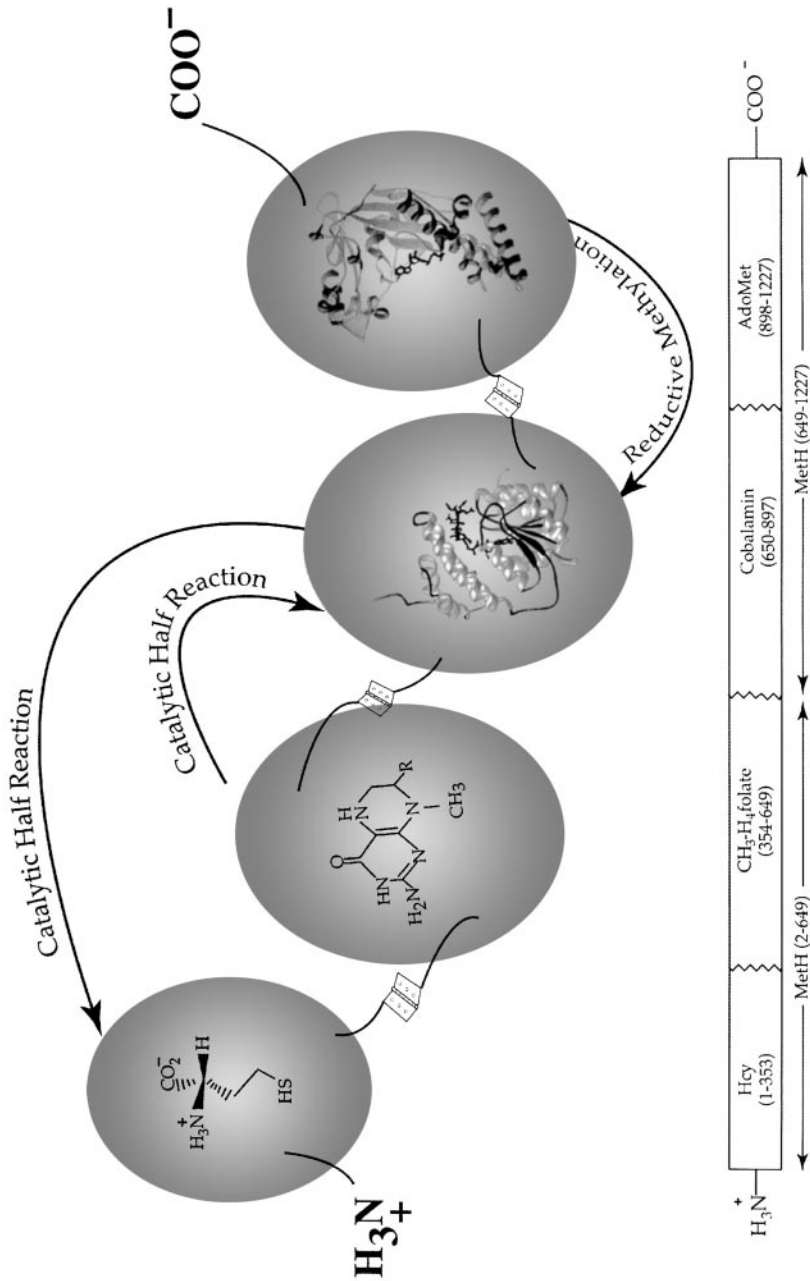
Figure 10 Reactions catalyzed by cobalamin-dependent methionine synthase. During the catalytic cycle, B$_{12}$ cycles between CH$_3$-Co(III) and Co(I). Occasionally, Co(I) undergoes oxidative inactivation to Co(II), which requires reductive activation. During reactivation, the methyl donor is AdoMet, and the electron donor is reduced flavodoxin in *E. coli* (78a) and methionine synthase reductase in humans (138).

carbohydrates and for fixing CO$_2$ and the toxic gas, CO. The key methyl donors are CH$_3$-H$_4$folate, methoxylated aromatics (CH$_3$-OAr), methanol, and CH$_3$-Co(III), although the important methyl acceptors are Co(I), and Ni(I) (Figure 8). The B$_{12}$-dependent reactions are catalyzed by CODH/ACS (AcsAB), vanillate O-demethylase (MtvABC), and the corrinoid iron-sulfur protein (AcsCD) (CFeSP) and its methyltransferase (AcsE) (Figure 9). These methyltransferase reactions feed into the central CO/CO$_2$ fixing and energy yielding metabolic pathway, which is called the Wood-Ljungdahl pathway (83).

CH$_3$-H$_4$folate is formed by a six- or four-electron reduction from CO$_2$ or CO, and the methyl group becomes the methyl of acetic acid (Figure 12). The CFeSP interfaces with two completely different types of proteins: a methyltransferase and CODH/ACS. The AcsE-methyltransferase catalyzes transfer of a methyl group from CH$_3$-H$_4$folate to the CFeSP, whereas the reaction with CODH/ACS involves methyl migration from the CFeSP presumably to Ni(I) in ACS. MeTr is a small dimeric protein containing two equivalent 33 kDa subunits and is a member of the TIM barrel protein family, which contains 8 beta strands and 8 alpha helices (84) (Figure 13A). AcsE-MeTr shares significant sequence homology with residues 340–580 of the *E. coli* methionine synthase where CH$_3$-H$_4$folate is presumed to bind (84). In AcsE-MeTr, CH$_3$-H$_4$folate binds within a negatively charged cleft in the alpha-beta barrel (85) (Figure 13B). Residues

A.

CO$_2$

H$_4$folate

CO$_2$
⟍CODH

ArO-CH$_3$

CO

CH$_3$-Co(III)

CoA

O-Demethylase
(MtvABC)

AcsE-MeTr

ACS

O

CH$_3$-H$_4$folate

Co(I)

SCoA

CFeSP

B.

CH$_3$OH
CH$_3$SR
CH$_3$NR$_2$

CO$_2$
↑CODH

MT1-MeTr↓E

CO

HSCoM   CH$_3$-Co(III)

H$_4$MPT   CH$_3$-Co(III)

CoA

MT2-MeTr╲D   MT1-MeTr╱C

MeTr╲B

ACS╱A   O

CH$_3$-CoM

Co(I)   CH$_3$-H$_4$MPT

Co(I)

SCoA
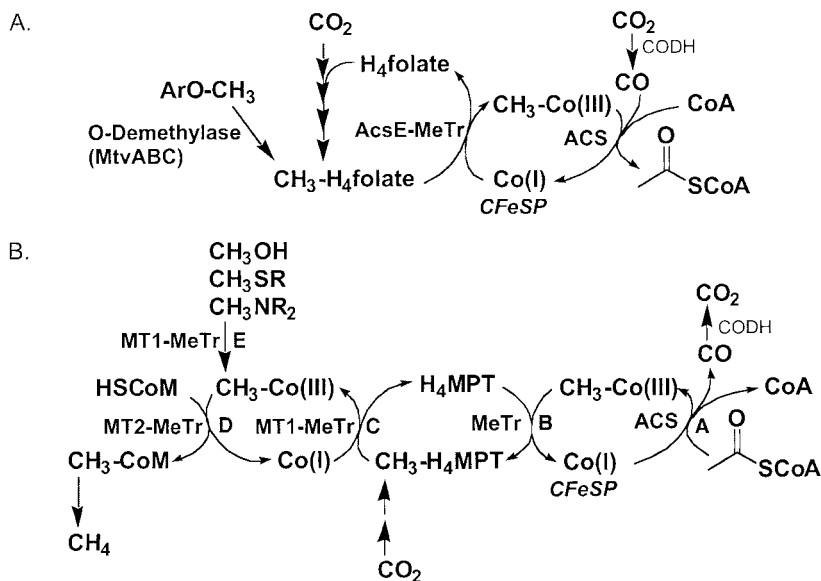
CH$_4$

CFeSP

CO$_2$

Figure 12   (*A*) The Wood-Ljungdahl Pathway. ACS, acetyl-CoA synthase; CODH, CO dehydrogenase; CFeSP, corrinoid iron-sulfur protein; and MeTr, AcsE-methyltransferase. (*B*) B$_{12}$-dependent methyltransferases in methanogenesis. The letters on the individual steps designate MeTr reactions that are discussed in the text.

D75, N96, and D160 interact with the pterin substrate in AcsE-MeTr and are strictly conserved in methionine synthase.

    After a role for cobamides was discovered in acetogenesis (86, 87), twenty years elapsed before the physiological methyl carrier, the CFeSP, was isolated (88). When this protein was purified to homogeneity and characterized, a modified form of B$_{12}$, 5′-methoxybenzimidazolylcobamide, and a [4Fe-4S]$^{2+/1+}$ cluster were found; thus the name corrinoid iron-sulfur protein was proposed (89). A distinguishing feature of the CFeSP is its base-off His-off conformation, i.e., neither the intramolecular benzimidazole base nor a protein-derived histidine residue coordinates to the cobalt in any of its redox states (89–91). The absence of a lower axial ligand is believed to be important for promoting heterolytic cleavage of the Co-C bond and disfavoring homolytic cleavage (89, 92).

Figure 11   Modular structure of methionine synthase. The four modules are connected by flexible linker regions, shown as hinges, that facilitate a molecular juggling act, which allows the CH$_3$-H$_4$folate-, AdoMet-, or homocysteine-binding domains to alternatively access the B$_{12}$-binding module. The region of the amino acid sequence comprising each module is shown below the diagram. From Figure 3 of (77).
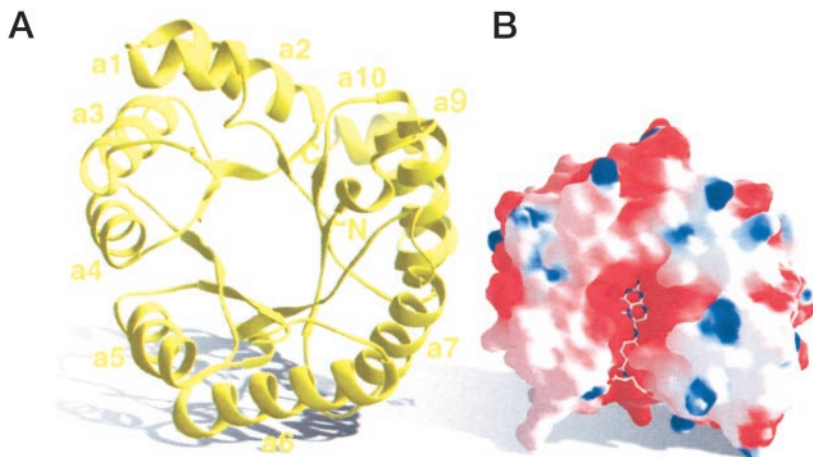
Figure 13   Structure of the AcsE-MeTr. (*A*) TIM barrel fold of the dimeric MeTr. (*B*) Electrostatic diagram showing CH$_3$-H$_4$folate binding within a negatively charged cleft in the TIM barrel.

Furthermore, removal of the lower axial ligand is correlated with an increase in the midpoint potential of the Co(II)/(I) couple by ca. 150 mV, which would favor the active Co(I) state within the cell (92).

O-DEMETHYLASES   Another B$_{12}$-dependent methyltransferase that is important to acetogenic microbes is the O-demethylase, which couples the demethylation of an aromatic methyl ether to the formation of CH$_3$-H$_4$folate (Figure 12) (93). Anaerobic cleavage of the methyl group in an O-demethylation reaction leaves the ether oxygen in the phenolic product (94), which is excreted. The methyl group is further metabolized by the Wood-Ljungdahl pathway (Figure 12*A*).

The proteins involved in the O-demethylation reaction are MtvA, -B, and -C, which are induced when *Moorella thermoacetica* is exposed to the phenyl-methylether (95). In this three-component system, MtvB binds the phenylmethyl-ether and catalyzes methyl transfer to form a CH$_3$-Co species bound to MtvC. MtvA binds H$_4$folate and catalyzes transmethylation from CH$_3$-Co(III) to form CH$_3$-H$_4$folate (96–99).

METHANOGENESIS AND B$_{12}$ In methanogens, the key methyl donors are CH$_3$-H$_4$MPT, methanol, protein-bound CH$_3$-Co(III), methylthiols, methylamines, and CH$_3$-SCoM, while the methyl acceptors are CoM, homocysteine, Co(I), and Ni(I) (Figure 8). The cobalamin-dependent reactions involve MtaABC, MtmABC, MttABC, MtsAB, MtrH, and CODH/ACS (CdhABC). The methanogenic methionine synthase at least in one methanogen appears to be a B$_{12}$-dependent enzyme (100).
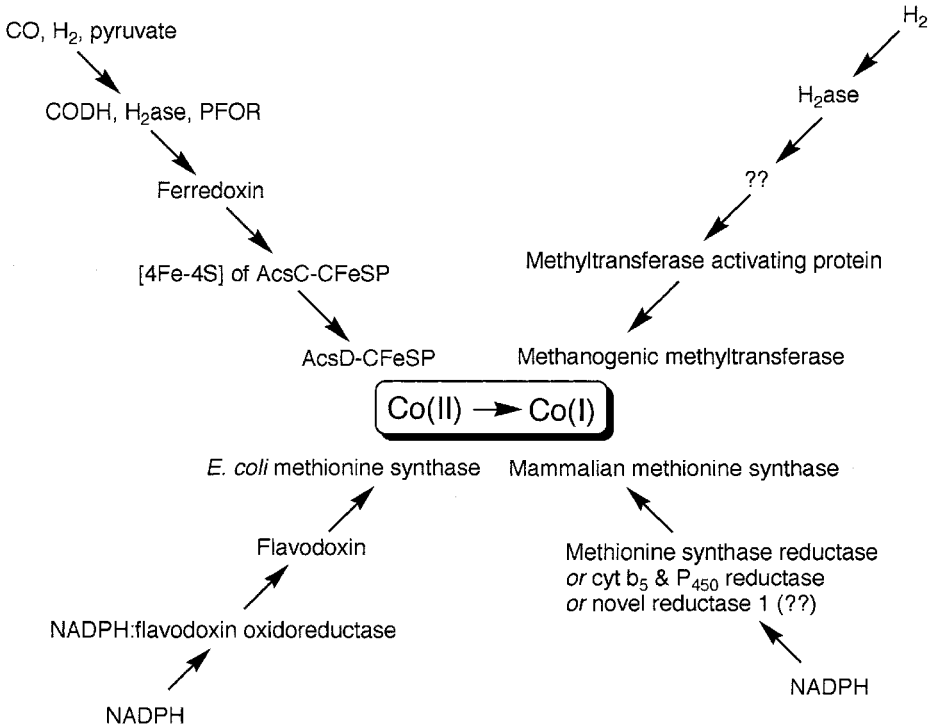
Figure 14   Different systems for activation of B$_{12}$-dependent methyltransferases.

Conversion of the methyl group of acetyl-CoA to methane by acetoclastic methanogens involves 4 methyl transfer steps (Figure 12*B*, Steps A–D). This reaction sequence is essentially the reverse of acetyl-CoA synthesis by acetogens (above). In methanogens, acetyl-CoA is disassembled by the bifunctional CODH/ACS (CdhABC) (Step A) (101) to form enzyme-bound intermediates (E-CO, E-SCoA, E-CH$_3$). CO undergoes oxidation and is released as CO$_2$, CoA is released into solution, and the methyl group is transferred first to a CFeSP and then to H$_4$MPT en route to methane (102, 103).

Methylotrophic methanogenesis denotes the generation of methane from simple methyl group donors like methanol, tri-, di-, and mono-methylamines and methylsulfides. Methylamines are important methane precursors in marine environments, where they arise from the breakdown of common osmolytes (104). Dimethylsulfide is responsible for up to 90% of the sea to air biogenic sulfur flux and is produced by marine phytoplankton as the main volatile sulfur compound emitted from the ocean (105). The methylotrophic MT1 enzymes catalyze transfer of the methyl group from methanol (MtaB), methylamines (MtbB and MttB), and methylthioethers (MtsB) to their specific cognate corrinoid proteins (106, 107) (Figure 9, reaction E in Figure 12*B*, and Figure 14). The MtmB structure (108)

reveals a TIM-barrel fold, like the AcsE-MeTr. An unusual feature of the methyl-amine methyltransferases is a novel amino acid, pyrolysine, which is encoded by a UAG codon within the coding regions of the *mtm*B, *mtb*B, and *mtt*B genes (109). MtsB of the methylthiol:CoM methyl transferase contains both the methanethiol-binding protein and its corrinoid protein on a single subunit (110), which, like all the corrinoid proteins involved in methylotrophic methanogenesis, is homologous to the B_{12}-binding domain of methionine synthase (106, 107, 110). The MT2-dependent methylation of CoM generates CH_3-SCoM, the direct methane precursor from all methanogenic substrates (112).

A novel bioenergetic mechanism is exhibited by the MT2-like component of the methyltetrahydromethanopterin:CoM methyltransferase (Mtr) (113). This membrane-bound enzyme contains 8-subunits (MtrA-H) and generates a sodium ion gradient, which is used to produce ATP (114, 115). The reaction involves the methylation of the Co(I) center in MtrA by MtrH [MtrH is homologous to the AcsE-MeTr (116)] followed by transfer of the methyl group from CH_3-cobalt to CoM by one of the components of the MtrA-H complex. The latter step is the energy-yielding component of the reaction (114).

Mechanism of Methyl Transfer

The key steps in the methyltransferase mechanism are substrate binding, activation of the methyl group to enhance its reactivity toward nucleophilic attack, activation/generation of the Co(I) nucleophile, the methyl group transfer reaction itself, and product release.

BINDING AND ACTIVATION OF THE METHYL GROUP AND METHYL GROUP DONOR CH_3-H_4folate binds tightly to the AcsE-MeTr from *M. thermoacetica* within a negatively charged region in the crevice (Figure 13*B*) of a TIM barrel structure (84). The *Methanosarcina barkeri* monomethylamine methyltransferase (MtmB) shares this TIM barrel fold (108) and, based on sequence homology with AcsE-MeTr (84), the CH_3-H_4folate binding domain of methionine synthase is predicted to also adopt this fold.

Methyl transfer from a tertiary amine requires activation of the methyl donor. Protonation at N5 is a plausible mechanism, which is consistent with the observed proton uptake during the reaction (117). This would lower the activation barrier to nucleophilic displacement of the methyl group by the Co(I) nucleophile. Proton transfer could occur either in the binary complex between enzyme and CH_3-H_4folate (117, 118) or later along the reaction coordinate (119). The second-order rate constant for the AcsE-MeTr-catalyzed reaction of CH_3-H_4folate and the CFeSP (120) or of methionine synthase (2-649) with exogenous cobalamin (77) increases as the pH is lowered; this exhibits an apparent pKa of 5.6–6.0. The reverse reactions exhibit the opposite pH-rate profile, with the second-order rate constant decreasing as the pH is lowered. Binding of CH_3-H_4folate to AcsE-MeTr results in proton uptake from solution (117), which

suggests protonation in the binary complex. However, the MetH (2-649) domain does not bind protonated CH$_3$-H$_4$folate, and proton release rather than proton uptake accompanies formation of the binary complex (119). Thus, while it is clear that general acid catalysis is involved in the methyl transfer reaction, whether this occurs in the binary complex, in the ternary complex (with the methyl acceptor), or in the transition state for the methyl transfer reaction remains open. Methionine synthase and AcsE-MeTr appear to differ in this aspect of catalysis.

Activation of the methyl group of other methyl donors (methanol, methyl amines, and methane thiols) is less well understood. Although one possibility is protonation, another is coordination of the heteroatom of the methyl donor substrate to a Lewis acid. Activation of methanol in the methanol methyltransferase system requires Zn (121), and ligation of methanol to the Zn^{2+} ion in the methanol methyltransferase system (81) is presumed to be important. Model studies support a role for Zn^{2+} in catalysis of methyl transfer to Co(I) (122).

In the MT2-type reactions involving transfer of the methyl group from CH$_3$-Co(III) (Figure 9), activation of the methyl acceptor is required. The substrates for methionine synthase and the CoM methyltransferases (homocysteine or CoM) are not very nucleophilic in their protonated state, which is the predominant form at physiological pH. For homocysteine, the thiol exhibits a microscopic pKa of 9.0 when the amino group is protonated (123). The pH-activity profile of the reaction of 2-mercaptoethanol with MeCbl indicates participation of the thiolate as a nucleophile (124). In the enzymatic system, the thiolate appears to be generated by ligation to an active-site Zn^{2+} (125). The homocysteine-binding module of methionine synthase contains a zinc ion, which is coordinated to three cysteine residues and one O/N ligand in its resting state (126). Homocysteine replaces the O/N ligand to form a tetrahedral Zn-S$_4$ site (127). Similarly, Zn-dependent activation appears to be important in MT2-type reactions involving transfer of the methyl group of CH$_3$-Co(III) to CoM (121, 128).

ACTIVATION OF COBALAMIN   Co(I) in B$_{12}$ is a supernucleophile, with a Pearson constant of 14 (129), and is weakly basic, with a pKa below 1 for the Co(I)-H complex (130). Thus, Co(I), with a free lone pair of electrons, is poised for nucleophilic attack on an activated methyl group. Co(I) is also highly reducing, with the redox potential for the Co(II)/(I) couple below -500 mV (92, 131, 132). These properties make Co(I) fairly unstable and easy to oxidize. In the anaerobic microbial system (AcsA-E), the cobalt center is oxidized to the inactive Co(II) state once in every 100 turnovers (133). In methionine synthase, oxidative inactivation is estimated to occur once every 2000 turnovers (134). Reductive reactivation is necessary for reentry to the catalytic cycle, a feature common to all the B$_{12}$-dependent methyltransferases. A number of different reactivation systems have evolved to accomplish this (Figure 14).

An important aspect of reactivation, which was first shown for the acetogenic CFeSP (89) and is probably shared among all B$_{12}$-dependent methyltransferases,
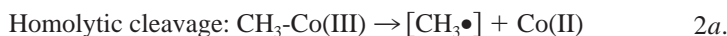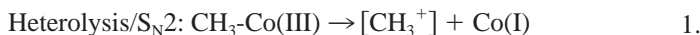
is that the cofactor adopts a base-off conformation. The base-off His-on conformation is found in many B_{12}-dependent methyltransferases (135), whose sequences contain a consensus motif (DX**H**XXG), where H represents the lower axial histidine ligand. In the acetogenic system, the Co(II) state of the CFeSP appears to already be four-coordinate, which facilitates electron transfer to form a four-coordinate Co(I) state (89–92). Electron transfer occurs from an external electron donor (CO, H_2, pyruvate) to an oxidoreductase (CODH, hydrogenase, pyruvate ferredoxin oxidoreductase), to a low-potential ferredoxin, to the [4Fe-4S] cluster in the AcsC subunit of the CFeSP, which transfers an electron to Co(II) (133).

Another pathway for reductive reactivation is exemplified by methionine synthase, where an unfavorable one-electron reduction of the inactive Co(II) to the Co(I) state is coupled to the highly exergonic demethylation of AdoMet to form MeCbl (136, 137). This is a striking example of how coupling of an unfavorable redox reaction to a highly favorable chemical reaction can markedly affect the apparent Co(II)/(I) redox potential (136). In *E. coli*, flavodoxin is the proximal electron donor, while in humans, the electron donor is methionine synthase reductase (138). Besides the requirement for a low potential electron donor, the lower axial histidine ligand to the cobalt of methionine synthase must be removed to facilitate reduction of the inactive Co(II) enzyme. A catalytic triad consisting of H759, D757, and S810 appears to facilitate removal of the axial histidine ligand by its protonation. Proton uptake is associated with reduction of Co(II) to Co(I) (139). In fact, binding of flavodoxin is sufficient to induce the conversion of 5- to 4-coordinate Co(II) (139), the coordination state naturally found in the Co(II) form of the acetogenic CFeSP. Generation of a 4-coordinate Co(II) complex also is an intermediate step in the electrochemical reduction to the Co(I) state of B_{12} in solution (139a).

A third ATP requiring activation system is exhibited by the MT2-type methanol- and methylamine-methyltransferases (140). A protein, which is called RamM, appears to contain two [4Fe-4S clusters] that are involved in catalyzing the ATP-dependent reductive activation of any of the methylamine MT2-type methyltransferases (Joseph Krzycki, personal communication). ATP-dependent activation also appears to be required for the aromatic O-demethylase from some acetogens (141).

THE METHYL TRANSFER: HETEROLYSIS VERSUS HOMOLYSIS, S_N2 VERSUS OXIDATIVE ADDITION   Theoretically, a methyl group can be transferred as a cation, radical, or anion (Equations 1–3). Although, of the reactions shown in Figure 8, only the methionine synthase and Wood-Ljungdahl pathway reactions have been studied in sufficient detail to assign the oxidation states of the reaction intermediates, it seems reasonable to conclude that all the methyltransferases share a common mechanism that involves transfer of the methyl group formally as a carbocation and cycling of the cobamide cofactor between Co(I) and CH_3-Co(III) (Equation 1). Transfer of a radical would involve a Co(II) intermediate, either in the

activation of the methyl group (Equation 2*B*) or after homolytic cleavage (Equation 2*A*). Mutagenesis, rapid kinetics, and single-turnover studies of the methyl transfer reactions in the Wood-Ljungdahl pathway indicate the absence of either Co(II) intermediates or electron transfer reactions during the catalytic cycle (120, 133, 142, 143). Additionally, there is no evidence for a methyl anion transfer, which would result in a Co(III) product or intermediate after Co-C bond cleavage (Equation 3).

$$\text{Heterolysis/S}_\text{N}\text{2: CH}_3\text{-Co(III)} \rightarrow [\text{CH}_3^+] + \text{Co(I)} \qquad 1.$$

$$\text{Homolytic cleavage: CH}_3\text{-Co(III)} \rightarrow [\text{CH}_3\bullet] + \text{Co(II)} \qquad 2a.$$

$$\text{Electron transfer/homolysis: CH}_3\text{-Co(III)}$$

$$+ \; 1 \; e^- \rightarrow \text{CH}_3\text{-Co(II)} \rightarrow [\text{CH}_3\bullet] + \text{Co(I)} \qquad 2b.$$

$$\text{Heterolysis: CH}_3\text{-Co(III)} \rightarrow [\text{CH}_3^-] + \text{Co(III)} \qquad 3.$$

The heterolytic cleavage of the Co-C bond could occur by an S$_\text{N}$2-type reaction or by an oxidative addition reaction (77). An S$_\text{N}$2 reaction (Figure 15*A*) involves back-side attack on the methyl group, which leads to inversion of configuration at carbon. This mechanism requires in-line geometry of the methyl group donor and the methyl group acceptor. The oxidative addition reaction (Figure 15*B*) is a ligand substitution or ligand interchange reaction in which the dz^2 orbital of the Co(I) initially bonds with the methyl carbon and with the heteroatom to which the CH$_3$ group is attached and would lead to retention of configuration at the transferred carbon. As pointed out by Matthews (77), the critical issue for an oxidative addition mechanism is whether CH$_3$-H$_4$folate can be positioned close enough to the corrin ring to afford the appropriate steric and symmetry interactions necessary for orbital overlap. The empty 4s cobalt orbital would hybridize with the symmetry-matched σ orbital of the C-N bond and the filled 3d$_{xz}$ or 3d$_{yz}$ cobalt orbital of the metal would hybridize with the empty σ* orbital of the C-N bond to weaken the N5-methyl bond of CH$_3$-H$_4$folate.

Stereochemical analyses of the overall reactions catalyzed by the Wood-Ljungdahl pathway (144) and by methionine synthase (145) are consistent with two consecutive S$_\text{N}$2-type reactions, i.e., transfer of the methyl group first to Co(I) and subsequently to the A-Cluster of ACS or to homocysteine respectively. However, the individual methyl transfer reactions, e.g., CH$_3$-H$_4$folate to acetyl-CoA (or methionine), have not been interrogated. Therefore, the stereochemical results for the overall reaction require that the MT1- and MT2-catalyzed half reactions occur by the same reaction mechanism, i.e., either two S$_\text{N}$2 or two ligand interchange reactions, because either would yield net retention of the stereochemical configuration. Crystallization of a binary complex of CH$_3$-H$_4$folate with intact methionine synthase or a ternary complex of CH$_3$-H$_4$folate with AcsE-MeTr and the CFeSP would illuminate the mechanism of methyl
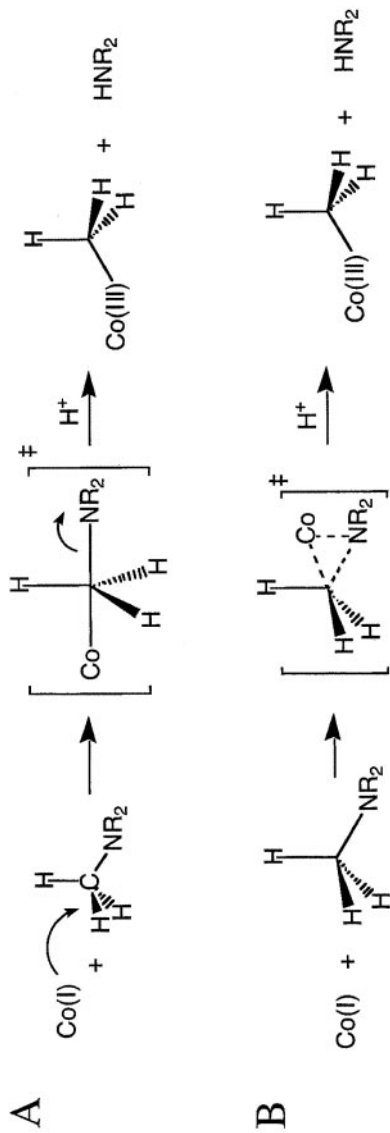
Figure 15   Comparison of S_N2 (*A*) and oxidative addition (*B*) mechanisms for methyltransferases.

transfer by revealing the relative orientations of cobalt, the methyl group, and the heteroatom attached to the methyl group.
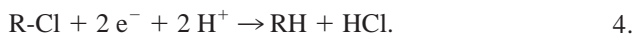
B$_{12}$-DEPENDENT REDUCTIVE DEHALOGENASES

Classes of Dehalogenases and Their Environmental Role

Anaerobic microbes containing B$_{12}$-dependent reductive dehalogenases play an important role in the detoxification of aromatic and aliphatic chlorinated organics, which include compounds on the EPA priority pollutant list such as chlorinated phenols, chlorinated ethenes, and PCBs (146, 147). Exposure to these compounds induces a host of genes involved in removing the chloride ion. Both aerobic and anaerobic microbes can perform dehalogenation; however, anaerobic bacteria are more efficient in removing halogen atoms from polyhalogenated compounds (148). *Desulfomonile tiedjei* was the first dehalogenating anaerobe to be isolated and characterized (149), and ~20 strains of anaerobic organisms capable of reductive dehalogenation have so far been isolated, including *Desulfomonile*, *Desulfitobacterium*, and *Dehalobacter*.

Substrate Specificity and Bioremediation

Organisms have distinct preference for the chlorine substituent they can remove; for example, *D. tiedjei* removes the *meta* chlorine group of chlorophenols and chlorobenzoates (149), while *Desulfitobacterium dehalogenans* (150), *Desulfitobacterium hafniense*, and *Desulfitobacterium chlororespirans* (151–153) dehalogenate at the position *ortho* to a hydroxy group. *D. dehalogenans* can also dehalogenate hydroxy-PCBs (154). On the other hand, *Desulfitobacterium frappieri* PCP-1 catalyzes dehalogenation of chlorophenols (155) or anilines with chlorine groups at the ortho, meta, and para positions. *D. tiedjei* also can dehalogenate trichloroethylene (156). The purified *D. chlororespirans* enzyme can catalyze the dechlorination of a hydroxy-PCB (3,3',5,5'-tetrachloro-4,4'-biphenyldiol) (153),

$$\text{R-Cl} + 2\,\text{e}^- + 2\,\text{H}^+ \rightarrow \text{RH} + \text{HCl}. \qquad 4.$$

There are two major classes of anaerobic dehalogenases: the heme containing 3-chlorobenzoate reductive dehalogenase from *D. tiedjei* (157) and the vitamin B$_{12}$-dependent enzymes. The B$_{12}$-dependent reductive dehalogenases, most of which also contain iron-sulfur clusters, are either embedded in or attached to the membrane by a small anchoring protein. This membrane association is important in linking the dehalogenation reaction to the electron transport pathway of anaerobic respiration.

The gene encoding the reductive dehalogenase (CprA) is embedded in a cluster of genes that encodes a membrane anchor (CprB), a membrane-associated regulatory protein (CprC), a DNA binding protein (CprK), and several chaper-

ones (CprT, CprD, CprB) (158). Several B_{12}-dependent dehalogenases have been purified, including the 3-chloro-4-hydroxy-phenylacetate reductive dehalogenases from *D. hafniense* (159) and *D. dehalogenans* (160), the 3-chloro-4-hydroxybenzo-ate dehalogenase from *D. chlororespirans* (153), and the haloalkane (perchloroeth-ylene and trichloroethene) dehalogenases from *Desulfitobacterium* strain PCE-S (161), *Dehalobacter restrictus* (162), and *Dehalobacter multivorans* (163, 164). These proteins contain a corrinoid, a [4Fe-4S] cluster, and a [3Fe-4S] cluster per monomeric unit. In some anaerobes, an unusual corrinoid cofactor appears to be present, because a recently isolated strain of *D. multivorans* that contains the standard corrinoids, but lacks the corrinoid cofactor that has been identified in the dehaloge-nase, is unable to dehalogenate TCE (165). Multiple dehalogenases are evident in the genome sequence of *D. hafniense* strain DCB-2 (166). Seventeen genes homologous to reductive dehalogenases are present in *Dehalococcoides ethenogenes* strain 195 (Steve Zinder, personal communication). Thus, the ability of certain dehalorespiring microbes to metabolize various types of chlorinated organic compounds (e.g., chloroalkanes plus chlorobenzoates) is conferred by separate (but homologous) enzymes (167).

Role of Cobalamin: Organometallic Adduct or Electron Transfer?

The role of B_{12} in the reductive dehalogenases appears to be significantly different from those of the AdoCbl-dependent isomerases and the MeCbl-dependent methyltransferases. Mechanistic studies on the anaerobic dehaloge-nases have lagged behind studies on the aerobic enzymes. Two working models for the mechanisms of dehalorespiring reductive dehalogenases are shown in Figure 16. In Path A, an organocobalt adduct is formed as in the methyltrans-ferases. In Path B, the corrinoid serves as an electron donor. In Path A, the halide is eliminated as the aryl-Co(III) intermediate is formed. Path B resembles the Birch reduction of hydroxylated aromatics in which a radical anion is formed. Both mechanisms assume that the corrinoid is the site of dehalogenation based on the ability of B_{12} to catalyze dehalogenation in solution (168) and light-reversible inhibition by propyl iodide, a characteristic of corrinoid-dependent reactions (162, 169). Because only low potential reductants can drive this reaction, Co(I) is likely to be the active species; however, none of the dehalogenases-bound intermediates shown in Figure 16 have been identified. When B_{12} is reacted with perchloroethylene, the Co(I) spectrum disappears as Co(II) is formed, and it is consistent with pathway B, which involves radical intermediates and Co(I) as an electron donor without an organocobalt intermediate. (170). Radical trap exper-iments provide further evidence for pathway B.

The k_{cat} for dehalogenation of 3-chloro-4-hydroxybenzoate by the *D. chlo-rorespirans* dehalogenase is 2.3-fold higher in 100% H_2O than in 100% ^2H_2O, and the proton inventory plot is linear, which indicates that a single proton is transferred in a partially rate limiting reaction in the dehalogenase mechanism (153). These results suggest deprotonation of an active-site water molecule,

Figure 16 Alternative mechanisms for reductive dehalogenation. Adapted from (153).

because deuterium from solvent is incorporated specifically into the carbon of 2,5-dichlorobenzoate that undergoes dehalogenation (171).

Energy Conservation by Dehalorespiration

Bacteria derive energy by dehalorespiration, which couples the dehalogenation reaction to an electron transfer chain. The energetics are favorable because low potential reductants like pyruvate, formate, or hydrogen, with redox potentials below -400 mV, donate electrons to fairly oxidizing electron acceptors (the RCl/RH couple are between $+250$ and $+600$ mV) (148, 172). For example, for perchloroethylene dechlorination, 189 kJ per mol of H_2, is available, equivalent to ~2.5 ATP. However, with pyruvate as the electron donor, only 1 mol of ATP or less per mol of chloride was removed (167, 173). This poor efficiency may reflect the recent evolution of the ability to metabolize these man-made compounds, most of which are not naturally produced.

Inhibition of dehalorespiration by uncouplers indicates a chemiosmotic ATP synthesis mechanism (174) and implies that the dehalogenase and the electron donating enzymes are membrane associated. The reductive dehalogenases appear to face the inside and the hydrogenases to face the outside of the cytoplasmic membrane (162, 175). A b-type cytochrome(s) (176) and menaquinone are believed to be involved in the electron transport chain (177).

Many fundamental questions regarding the reaction mechanism of dehalogenases remain. Are organocobalt adducts analogous to those in B_{12}-dependent methyltransferases formed? How is the chloride replaced by a hydride equivalent? Does the reaction involve radical intermediates? A hurdle in mechanistic studies has been the very poor growth of the organisms, which results in very low amounts of protein to investigate. Development of better strategies for growth of the organisms and/or heterologous expression of the genes will be a boon to this field.

ACKNOWLEDGMENTS

The *Annual Review of Biochemistry* is online at http://biochem.annualreviews.org

LITERATURE CITED

1. Whipple GH, Robscheit-Robbins FS. 1926. *Am. J. Physiol.* 72:408–18
2. Minot GR, Murphy WP. 1926. *JAMA* 87:470–76
3. Smith EL. 1948. *Nature* 161:638
4. Rickes EL, Brink NG, Konivszy FR, Wood TR, Folkers K. 1948. *Science* 107:396–97
5. Hodgkin DC, Kamper J, Mackay M, Pickworth JW, Trueblood KN, White JG. 1956. *Nature* 178:64
5a. Stevens R. 1982. In B_{12}, Vol. 1, ed. D.

Dolphin, pp. 169–200. New York: Wiley

6. Barker HA, Weissbach H, Smyth RD. 1958. *Proc. Natl. Acad. Sci. USA* 44:1093–97

7. Guest JR, Friedman S, Woods DD, Smith EL. 1962. *Nature* 195:340–42

8. Banerjee R. 1997. *Chem. Biol.* 4:175–86

9. Banerjee R. 2001. *Biochemistry* 40:6191–98

10. Marsh EN, Drennan CL. 2001. *Curr. Opin. Chem. Biol.* 5:499–505

11. Brown KL, Hakimi JM. 1984. *J. Am. Chem. Soc.* 106:7894–99

12. Mancia F, Keep NH, Nakagawa A, Leadlay PF, McSweeney S, et al. 1996. *Structure* 4:339–50

13. Reitzer R, Gruber K, Jogl G, Wagner UG, Bothe H, et al. 1999. *Struct. Fold. Des.* 7:891–902

14. Marsh ENG, Holloway DE. 1992. *FEBS Lett.* 10:167–70

15. Shibata N, Masuda J, Tobimatsu T, Toraya T, Suto K, et al. 1999. *Struct. Fold. Des.* 7:997–1008

16. Sintchak MD, Arjara G, Kellogg BA, Stubbe J, Drennan CL. 2002. *Nat. Struct. Biol.* 9:293–300

17. Ke SC, Torrent M, Museav DG, Morokuma K, Warncke K. 1999. *Biochemistry* 38:12681–89

18. Abend A, Bandarian V, Nitsche R, Stupperich E, Retey J, Reed GH. 1999. *Arch. Biochem. Biophys.* 370:138–41

19. Finke RG, Hay BP. 1984. *Inorg. Chem.* 23:3041–43

20. Hay BP, Finke RG. 1987. *J. Am. Chem. Soc.* 109:8012–18

21. Brown KL, Zou X. 1999. *J. Inorg. Biochem.* 77:185–95

22. Halpern J. 1985. *Science* 227:869–75

23. Grate JH, Schrauzer GN. 1979. *J. Am. Chem. Soc.* 101:4601–11

24. Marzilli LG, Toscano J, Randaccio L, Bresciani-Pahor N, Calligaris M. 1979. *J. Am. Chem. Soc.* 101:6754–56

25. Krouwer JS, Holmquist B, Kipnes RS, Babior BM. 1980. *Biochim. Biophys. Acta* 612:153–59

26. Glusker JP. 1982. See Ref. 5a, pp. 23–106

27. Dong S, Padmakumar R, Maiti N, Banerjee R, Spiro TG. 1998. *J. Am. Chem. Soc.* 120:9947–48

28. Huhta MS, Chen HP, Hemann C, Hille CR, Marsh EN. 2001. *Biochem. J.* 355:131–37

29. Padmakumar R, Padmakumar R, Banerjee R. 1997. *Biochemistry* 36:3713–18

30. Chowdhury S, Banerjee R. 2000. *J. Am. Chem. Soc.* 122:5417–18

31. Marsh ENG, Ballou DP. 1998. *Biochemistry* 37:11864–72

32. Bandarian V, Reed GH. 2000. *Biochemistry* 39:12069–75

33. Booker S, Licht S, Broderick J, Stubbe J. 1994. *Biochemistry* 33:12676–85

34. Essenberg MK, Frey PA, Abeles RH. 1971. *J. Am. Chem. Soc.* 93:1242–51

35. Weisblat DA, Babior BM. 1971. *J. Biol. Chem.* 246:6064–71

36. Chih HW, Marsh EN. 2001. *Biochemistry* 40:13060–67

37. Gerfen GJ. 1999. In *Chemistry and Biochemistry of B$_{12}$*, ed. R. Banerjee, pp. 165–95. New York: Wiley

38. Buettner GR, Coffman RE. 1977. *Biochim. Biophys. Acta* 480:495–505

39. Schepler KL, Dunham WR, Sands RH, Fee JA, Abeles RH. 1975. *Biochim. Biophys. Acta* 97:510–18

40. Licht S, Gerfen GJ, Stubbe J. 1996. *Science* 271:477–81

41. Bothe H, Darley DJ, Albracht SP, Gerfen GJ, Golding BT, Buckel W. 1998. *Biochemistry* 37:4105–13

42. Michel C, Albracht SP, Buckel W. 1992. *Eur. J. Biochem.* 205:767–73

43. Zelder O, Buckel W. 1993. *Biol. Chem. Hoppe-Seyler* 374:85–90

44. Zhao Y, Abend A, Kunz M, Such P, Retey J. 1994. *Eur. J. Biochem.* 225:891–96

..
..

45. Padmakumar R, Banerjee R. 1995. *J. Biol. Chem.* 270:9295–300

46. Gerfen GJ, Licht S, Willems J-P, Hoffman BM, Stubbe J. 1996. *J. Am. Chem. Soc.* 118:8192–97

47. Masuda J, Shibata N, Morimoto Y, Toraya T, Yasuoka N. 2000. *Struct. Fold. Des.* 8:775–88

48. Gruber K, Reitzer R, Kratky C. 2001. *Angew. Chem. Int. Ed. Engl.* 40: 3377–80

49. LoBrutto R, Bandarian V, Magnusson OT, Chen X, Schramm VL, Reed GH. 2001. *Biochemistry* 40:9–14

50. Warncke K, Utada AS. 2001. *J. Am. Chem. Soc.* 123:8564–72

51. Retey J, Arigoni D. 1966. *Experientia* 22:783–4

52. Toraya T, Yoshizawa K, Eda M, Yamabe T. 1999. *J. Biochem.* 126:650–54

53. Smith DM, Golding BT, Radom L. 2001. *J. Am. Chem. Soc.* 123:1664–75

54. Toraya T, Eda M, Kamachi T, Yoshizawa K. 2001. *J. Biochem.* 130: 865–72

55. Smith DM, Golding BT, Radom L. 1999. *J. Am. Chem. Soc.* 121:1383–84

56. Smith DM, Golding BT, Radom L. 1999. *J. Am. Chem. Soc.* 121:9388–99

57. Maiti N, Widjaja L, Banerjee R. 1999. *J. Biol. Chem.* 274:32733–37

58. Thoma NH, Evans PR, Leadlay PF. 2000. *Biochemistry* 39:9213–21

59. Chih H-W, Marsh ENG. 2000. *J. Am. Chem. Soc.* 122:10732–33

60. Wetmore SD, Smith DM, Golding BT, Radom L. 2001. *J. Am. Chem. Soc.* 123:7963–72

61. Madhavapeddi P, Marsh EN. 2001. *Chem. Biol.* 8:1143–49

62. Chang CH, Frey PA. 2000. *J. Biol. Chem.* 275:106–14

63. Chen HP, Wu SH, Lin YL, Chen CM, Tsay SS. 2001. *J. Biol. Chem.* 276: 44744–50

64. Frey PA, Chang CH. 1999. See Ref. 37, pp. 835–57

65. Wetmore SD, Smith DM, Radom L. 2000. *J. Am. Chem. Soc.* 122:10208–9

66. Tang KH, Chang CH, Frey PA. 2001. *Biochemistry* 40:5190–99

67. Magnusson OT, Frey PA. 2002. *Biochemistry* 41:1695–702

68. Huhta MS, Ciceri D, Golding BT, Marsh EN. 2002. *Biochemistry* 41: 3200–6

69. Pawelkiewicz J, Zagalak B. 1965. *Acta Biochim. Pol.* 12:207–18

70. Toraya T, Shirakashi T, Kosuga T, Fukui S. 1976. *Biochem. Biophys. Res. Commun.* 69:475–80

71. Poznanskaya AA, Yakusheva MI, Yakovlev VA. 1977. *Biochim. Biophys. Acta* 484:236–43

72. Honda S, Toraya T, Fukui S. 1980. *J. Bacteriol.* 143:1458–65

73. Ushio K, Honda S, Toraya T, Fukui S. 1982. *J. Nutr. Sci. Vitaminol.* 28:225–36

74. Mori K, Tobimatsu T, Hara T, Toraya T. 1997. *J. Biol. Chem* 272:32034–41

75. Tobimatsu T, Kajiura H, Yunoki M, Azuma M, Toraya T. 1999. *J. Bacteriol.* 181:4110–13

76. Mori K, Toraya T. 1999. *Biochemistry* 38:13170–78

77. Matthews RG. 2001. *Acc. Chem. Res.* 34:681–89

78. Matthews RG. 1999. See Ref. 37, pp. 681–706

78a. Fujii K, Huennekens FM. 1974. *J. Biol. Chem.* 249:6745–53

79. Goulding CW, Postigo D, Matthews RG. 1997. *Biochemistry* 36:8082–91

80. Drennan CL, Huang S, Drummond JT, Matthews RG, Ludwig ML. 1994. *Science* 266:1669–74

81. Sauer K, Thauer RK. 1999. See Ref. 37, pp. 655–80

82. Ragsdale SW. 1999. See Ref. 37, pp. 633–54

83. Ragsdale SW, Kumar M, Zhao S, Menon S, Seravalli J, Doukov T. 1998. In *Vitamin B$_{12}$ and B$_{12}$-Proteins*, ed. B

Krautler, pp. 167–77. Weinheim, Ger.: Wiley-VCH

84. Doukov T, Seravalli J, Stezowski J, Ragsdale SW. 2000. *Structure* 8: 817–30

85. Doukov T, Seravalli J, Ragsdale SW, Drennan CL. 2003. *Science* 298:567–72

86. Ljungdahl L, Irion E, Wood HG. 1966. *Fed. Proc.* 25:1642–48

87. Poston JM, Kuratomi K, Stadtman ER. 1964. *Ann. NY Acad. Sci.* 112:804–6

88. Hu S-I, Pezacka E, Wood HG. 1984. *J. Biol. Chem.* 259:8892–97

89. Ragsdale SW, Lindahl PA, Münck E. 1987. *J. Biol. Chem.* 262:14289–97

90. Wirt MD, Kumar M, Ragsdale SW, Chance MR. 1993. *J. Am. Chem. Soc.* 115:2146–50

91. Wirt MD, Wu J-J, Scheuring EM, Kumar M, Ragsdale SW, Chance MR. 1995. *Biochemistry* 34:5269–73

92. Harder SA, Lu W-P, Feinberg BF, Ragsdale SW. 1989. *Biochemistry* 28: 9080–87

93. Frazer AC. 1994. In *Acetogenesis*, ed. HL Drake, pp. 445–83. New York: Chapman & Hall

94. DeWeerd KA, Saxena A, Nagle DP Jr, Suflita JM. 1988. *Appl. Environ. Microbiol.* 54:1237–42

95. Naidu D, Ragsdale SW. 2001. *J. Bacteriol.* 183:3276–81

96. Berman MH, Frazer AC. 1992. *Appl. Environ. Microbiol.* 58:925–31

97. Meßmer M, Reinhardt S, Wohlfarth G, Diekert G. 1996. *Arch. Microbiol.* 165: 18–25

98. El Kasmi A, Rajasekharan S, Ragsdale SW. 1994. *Biochemistry* 33:11217–24

99. Kaufmann F, Wohlfarth G, Diekert G. 1997. *Arch. Microbiol.* 168:136–42

100. Schroder I, Thauer RK. 1999. *Eur. J. Biochem.* 263:789–96

101. Maupin-Furlow JA, Ferry JG. 1996. *J. Bacteriol.* 178:6849–56

102. Jablonski PE, Lu WP, Ragsdale SW, Ferry JG. 1993. *J. Biol. Chem.* 268: 325–29

103. Abbanat DR, Ferry JG. 1991. *Proc. Natl. Acad. Sci. USA* 88:3272–76

104. King GM. 1984. *Geomicrobiol. J.* 3:276–301

105. Charlson RJ, Schwartz SE, Hales JM, Cess RD, Coakely JA, et al. 1992. *Science* 255:423–30

106. Burke SA, Lo SL, Krzycki JA. 1998. *J. Bacteriol.* 180:3432–40

107. Sauer K, Harms U, Thauer RK. 1997. *Eur. J. Biochem.* 243:670–77

108. Hao B, Gong W, Ferguson TK, James CM, Krzycki JA, Chan MK. 2002. *Science* 296:1462–66

109. Paul L, Ferguson DJ, Krzycki JA. 2000. *J. Bacteriol.* 182:2520–29

110. Tallant TC, Krzycki JA. 1997. *J. Bacteriol.* 179:6902–11

111. Deleted in proof

112. Thauer RK. 1998. *Microbiology* 144: 2377–406

113. Gottschalk G, Thauer RK. 2001. *Biochim. Biophys. Acta* 1505:28–36

114. Weiss DS, Gartner P, Thauer RK. 1994. *Eur. J. Biochem.* 226:799–809

115. Harms U, Weiss DS, Gartner P, Linder D, Thauer RK. 1995. *Eur. J. Biochem.* 228:640–48

116. Hippler B, Thauer RK. 1999. *FEBS Lett.* 449:165–68

117. Seravalli J, Shoemaker RK, Sudbeck MJ, Ragsdale SW. 1999. *Biochemistry* 38: 5736–45

118. Seravalli J, Zhao S, Ragsdale SW. 1999. *Biochemistry* 38:5728–35

119. Smith AE, Matthews RG. 2000. *Biochemistry* 39:13880–90

120. Zhao S, Roberts DL, Ragsdale SW. 1995. *Biochemistry* 34:15075–83

121. Sauer K, Thauer RK. 1997. *Eur. J. Biochem.* 249:280–85

122. Schnyder A, Darbre T, Keese R. 1998. *Angew. Chem. Int. Ed. Engl.* 37: 1283–85

123. Reuben DME, Bruice TC. 1976. *J. Am. Chem. Soc.* 98:114–21

124. Hogenkamp HP, Bratt GT, Sun SZ. 1985. *Biochemistry* 24:6428–32

125. Matthews RG, Goulding CW. 1997. *Curr. Opin. Chem. Biol.* 1:332–39

126. Goulding CW, Matthews RG. 1997. *Biochemistry* 36:15749–57

127. Peariso K, Zhou ZS, Smith AE, Matthews RG, Penner-Hahn JE. 2001. *Biochemistry* 40:987–93

128. Leclerc GM, Grahame DA. 1996. *J. Biol. Chem.* 271:18725–31

129. Schrauzer GN, Deutsch E, Windgassen RJ. 1968. *J. Am. Chem. Soc.* 90:2441–42

130. Tackett SL, Collat JW, Abbott JC. 1963. *Biochemistry* 2:919–23

131. Lexa D, Savéant J-M, Zickler J. 1977. *J. Am. Chem. Soc.* 99:2786–90

132. Banerjee RV, Frasca V, Ballou DP, Matthews RG. 1990. *Biochemistry* 29:11101–9

133. Menon S, Ragsdale SW. 1999. *J. Biol. Chem.* 274:11513–18

134. Drummond JT, Huang S, Blumenthal RM, Matthews RG. 1993. *Biochemistry* 32:9290–95

135. Drennan CL, Matthews RG, Ludwig ML. 1994. *Curr. Opin. Struct. Biol.* 4:919–29

136. Banerjee RV, Harder SR, Ragsdale SW, Matthews RG. 1990. *Biochemistry* 29:1129–35

137. Jarrett JT, Hoover DM, Ludwig ML, Matthews RG. 1998. *Biochemistry* 37:12649–58

138. Olteanu H, Banerjee R. 2001. *J. Biol. Chem.* 276:35558–63

139. Hoover DM, Jarrett JT, Sands RH, Dunham WR, Ludwig ML, Matthews RG. 1997. *Biochemistry* 36:127–38

139a. Lexa D, Saveant JM. 1983. *Acc. Chem. Res.* 16:235–43

140. Wassenaar RW, Keltjens JT, van der Drift C. 1998. *Eur. J. Biochem.* 258:597–602

141. Kaufmann F, Wohlfarth G, Diekert G. 1998. *Eur. J. Biochem.* 253:706–11

142. Seravalli J, Kumar M, Ragsdale SW. 2002. *Biochemistry* 41:1807–19

143. Menon S, Ragsdale SW. 1998. *Biochemistry* 37:5689–98

144. Lebertz H, Simon H, Courtney LF, Benkovic SJ, Zydowsky LD, et al. 1987. *J. Am. Chem. Soc.* 109:3173–74

145. Zydowsky LD, Courtney LF, Frasca V, Kobayashi K, Shimizu H, et al. 1986. *J. Am. Chem. Soc.* 108:3152–53

146. Copley SD. 1998. *Curr. Opin. Chem. Biol.* 2:613–17

147. Janssen DB, Oppentocht JE, Poelarends GJ. 2001. *Curr. Opin. Biotechnol.* 12:254–58

148. El Fantroussi S, Naveau H, Agathos SN. 1998. *Biotechnol. Prog.* 14:167–88

149. Linkfield TG, Tiedje JM. 1990. *J. Ind. Microbiol.* 5:9–15

150. Utkin I, Dalton DD, Wiegel J. 1995. *Appl. Environ. Microbiol.* 61:346–51

151. Christiansen N, Ahring BK. 1996. *Int. J. Syst. Bacteriol.* 46:442–48

152. Sanford R, Cole J, Loffler F, Tiedje J. 1996. *Appl. Environ. Microbiol.* 62:3800–8

153. Krasotkina J, Walters T, Maruya KA, Ragsdale SW. 2001. *J. Biol. Chem.* 276:40991–97

154. Wiegel J, Zhang X, Wu Q. 1999. *Appl. Environ. Microbiol.* 65:2217–21

155. Dennie D, Gladu I, Lepine F, Villemur R, Bisaillon J, Beaudet R. 1998. *Appl. Environ. Microbiol.* 64:4603–6

156. Cole JR, Fathepure BZ, Tiedje JM. 1995. *Biodegradation* 6:167–72

157. Ni S, Fredrickson JK, Xun L. 1995. *J. Bacteriol.* 177:5135–39

158. Smidt H, van Leest M, van der Oost J, de Vos WM. 2000. *J. Bacteriol.* 182:5683–91

159. Christiansen N, Ahring BK, Wohlfarth G, Diekert G. 1998. *FEBS Lett.* 436:159–62

160. van de Pas BA, Smidt H, Hagen WR, van der Oost J, Schraa G, et al. 1999. *J. Biol. Chem.* 274:20287–92

161. Miller E, Wohlfarth G, Diekert G. 1998. *Arch. Microbiol.* 169:497–502

162. Miller E, Wohlfarth G, Diekert G. 1997. *Arch. Microbiol.* 168:513–19

163. Neumann A, Wohlfarth G, Diekert G. 1996. *J. Biol. Chem.* 271:16515–19

164. Neumann A, Wohlfarth G, Diekert G. 1998. *J. Bacteriol.* 180:4140–45

165. Siebert A, Neumann A, Schubert T, Diekert G. 2002. *Arch. Microbiol.* 178: 443–49

166. genome_hafniense. *http://www.jgi.doe.gov/JGI_microbial/html/desulfito/desulf_homepage.html*

167. van de Pas BA, Gerritse J, de Vos WM, Schraa G, Stams AJ. 2001. *Arch. Microbiol.* 176:165–69

168. Krone UE, Thauer RK, Hogenkamp HPC. 1989. *Biochemistry* 28:4908–14

169. Neumann A, Wohlfarth G, Diekert G. 1995. *Arch. Microbiol.* 163:276–81

170. Shey J, van der Donk WA. 2000. *J. Am. Chem. Soc.* 122:12403–4

171. Griffith GD, Cole JR, Quensen JF, Tiedje JM. 1992. *Appl. Environ. Microbiol.* 58:409–11

172. Dolfing J, Harrison BK. 1992. *Environ. Sci. Technol.* 26:2213–18

173. Holliger C, Hahn D, Harmsen H, Ludwig W, Schumacher W, et al. 1998. *Arch. Microbiol.* 169:313–21

174. Mohn WW, Tiedje JM. 1991. *Arch. Microbiol.* 157:1–6

175. Miller E, Wohlfarth G, Diekert G. 1997. *Arch. Microbiol.* 166:379–87

176. Holliger C, Wohlfarth G, Diekert G. 1999. *FEMS Rev.* 22:383–98

177. Schumacher W, Holliger C. 1996. *J. Bacteriol.* 178:2328–33